

Honours Dissertation



School of Science

Synthesis of Enzyme Inspired Immobilized Catalysts

Marc Agujar Malingin

A dissertation submitted in partial fulfilment

of the requirements for the degree of

Bachelor of Science (Honours)

Auckland University of Technology

16th of September 2023

ABSTRACT

The primary objective of this study is to develop an immobilized catalyst for transphosphorylation, drawing inspiration from enzymatic processes. To accomplish this goal, a set of key objectives were set. Firstly, the synthesis of TACN (A) and guanidinium (B) ligands is paramount. Then, the next objective is to immobilize these ligands onto a solid resin, establishing a bioactive site through a copper-catalyzed azide-alkyne cycloaddition (CuAAC) "click reaction." Lastly, the study aims to evaluate the catalytic activity of these supported catalysts using the model substrate HPNPP. This assessment seeks to identify optimal conditions for catalytic activation and to elucidate potential cooperativity in the catalytic process.

The focus of this project lies in investigating the catalytic properties of the selected ligands when immobilized on solid resin as an alternative to gold nanoparticles. The investigation includes the characterization of molecules, monitoring reactions through NMR and IR spectroscopy, and evaluating catalytic activity using UV-vis spectroscopy.

TACN (A) was initially synthesized using a protective group, Boc, and this was employed to selectively perform a substitution reaction at the desired site. Subsequently, "click chemistry" was utilized to attach it to the resin. Finally, the protective group was cleaved under acidic conditions.

The synthesis of Guanidinium (B) was approached through three distinct routes. The first route involved a standard substitution reaction, followed by a Staudinger reduction reaction, ending in guanylation. In the second route, with the aim of enhancing efficiency and effectiveness, a different starting material was used and tosylation was performed before following the aforementioned steps. The third route employed a completely different route, employing Gabriel synthesis to obtain the amine, which was eventually subjected to guanylation. Similar to the TACN synthesis, the "click reaction" was employed to immobilize the ligands, and deprotection was achieved through acidic conditions.

Honours Dissertation

We successfully showcased the immobilization of different functional groups onto the Merrifield resin's surface, resulting in the creation of a highly efficient transphosphodiesterase. This achievement holds promise for applications in synthesizing artificial enzymes characterized by great stability compared to their biological counterparts, along with the convenience of recovery and reusability. Our future research endeavors will focus on further enhancing this technology by exploring combinations of the two existing ligands and potentially introducing additional ligands in varying proportions, with the aim of developing artificial enzymes boasting even greater catalytic activities.

Table of content

Abstract	2
Abbreviations	7
List of Figures	9
List of Schemes	10
List of Tables	11
Attestation of Authorship	12
Acknowledgements	13
CHAPTER ONE: INTRODUCTION	14
1.1 Bioinspired catalysis.....	15
1.2 Benefits of modular assembled catalysis	17
1.3 System of interest	18
1.4 Aim of the research	25
CHAPTER TWO: RESULTS AND DISCUSSION	28
2.0 Overview	28
2.1 Synthesis of di- <i>tert</i> -Butyl 7-(pent-1-yn-5-yl)-1,4,7-triazacyclononane-1,4-dicarboxylate.....	29
2.2 Synthesis of 5-(<i>N,N'</i> -Bis(<i>tert</i> -butoxycarbonyl)- <i>N''</i> -butylguanidinyl)-pent-1- yne.....	31
2.3.0 Synthesis of Immobilized Catalyst.....	33
2.3.1 Synthesis of Merrifield resin	33

2.3.2 Immobilizing ligands via CuAAC click reaction.....	36
2.4.0 Optimizations of Synthetic routes.....	39
2.4.1 Obtaining Guanidinium substrate.....	39
2.4.2 Pre-immobilized halides.....	44
2.5.0 Preliminary kinetic analysis of synthesized catalysis on HPNPP via UV-Vis.....	46
2.5.1 Examining the optima type of buffer and pH.....	50
2.5.2 Transphosphorylation of HPNN using TACN-derivatised and Guanidinium-derivatised Merrifield resins.....	53
2.6 Conclusion and future work.....	55
CHAPTER THREE: EXPERIMENTAL.....	56
3.1 General details.....	56
3.2 Synthesis of Ligand A	57
3.2.1 Synthesis of Di- <i>tert</i> -butyl 1,4,7-triazacyclononane-1,4-dicarboxylate.....	58
3.2.2 Synthesis of di- <i>tert</i> -Butyl 7-(pent-1-yn-5-yl)-1,4,7-triazacyclononane-1,4-dicarboxylate.....	58
3.3.0 Synthesis of Ligand B.....	59
3.3.1 Synthesis of 5-Aminopent-1-yne.....	59
3.3.2 Synthesis of 6-tosylhex-1-yne.....	60
3.3.3 Synthesis of 6-azidohex-1-yne.....	61
3.3.4 Synthesis of 6-Aminohex-1-yne.....	62
3.3.5 Synthesis of 6-(<i>N,N</i> -Bis(<i>tert</i> -butoxycarbonyl)- <i>N</i> '-butylguanidiny)-hex-1-yne.....	63
3.3.6 Synthesis of 2-(hex-1-yn-6-yl)phthalimide.....	64
3.4.0 Synthesis of Merrifield resins, click reactions and deprotections.....	65

Honours Dissertation

3.4.1 Synthesis of benzyl azide.....	65
3.4.2 Synthesis of 1-benzyl-4-(1-chloropro-3-yl)-1,2,3-triazole.....	66
3.4.3 Synthesis of Azide-derivatised Merrifield resin (azidomethyl polystyrene).....	67
3.4.4 Synthesis of Model click-derivatised Merrifield resin.....	68
3.4.5 Synthesis diBocTACN-derivatised Merrifield resin.....	69
3.4.6 Synthesis of TACN-derivatised Merrifield resin.....	70
3.4.7 Synthesis of diBoc-guanidinium-derivatised Merrifield resin.....	71
3.4.8 Synthesis Guanidinium-derivatised Merrifield resin.....	72
References	73
Appendices	75

Abbreviations

°C	degrees Celsius
μM	micromolar
δ	chemical shift
π	pi
Boc	tert-butyloxycarbonyl
BORAX	Na ₂ B ₄ O ₇
CHES	2-(N-cyclohexylamino)ethanesulfonic acid
cm ⁻¹	wavelength
CuAAC	Copper-Catalyzed Azide-Alkyne Cycloaddition
d	doublet
DNA	deoxyribonucleic acid
HEPES	2-[4-(2-hydroxyethyl)piperazin-1-yl]ethanesulfonic acid
HPNPP	2-hydroxypropyl p-nitrophenyl phosphate
Hz	hertz
IR	infrared
J	coupling constant
m	multiplet
M s ⁻¹	moles per second
MHz	megahertz
mL	milliliters
mmol	millimole(s)

Honours Dissertation

NMR	nuclear magnetic resonance
PNP	<i>p</i> -nitrophenolate
ppm	parts per million
RNA	ribonucleic acid
S	singlet
TACN	1,4,7-triazacyclononane
TLC	Thin Layer Chromatography
UV-Vis	ultraviolet-visible

List of Figures

Figure 1: Basic representation of how enzymes catalyze reactions.

Figure 2: Different strategies for increasing the activity of cooperative catalysts (left to right; b hydrophobic interactions, molecular scaffold, dendrimers, attachment onto surface, hydrogen bonding)

Figure 3: Examples of different catalysis models

Figure 4: Nanozymes created by Manea and co-workers

Figure 5: Cooperative artificial catalyst system demonstrating covalently-bound system (top) and self-assembly (bottom).

Figure 6: Swelling of resins to allow access of solvent and reagents (A), representation of the parts of the resin (B), examples of different types of resins (C).

Figure 7: Hydrolysis of HPNPP and proposed transition state, used an RNA cleavage model.

Figure 8: Representation of how the Merrifield resin behaves under MeOH/DMSO (left) and CH_2Cl_2

Figure 9: IR spectra of Azide-derivatised resin (red) and post-“click” hydroxy-derivatised resin (green)

Figure 10: Post-“click” hydroxy-derivatised resin (pink) and post-“click” bromide-derivatised resin

Figure 11: Model click-derivatised Merrifield resin (red) and post-“click” phthalamide-derivatised resin

Figure 12: Initial rate of HPNPP hydrolysis at different pH level

Figure 13: Initial rate of HPNPP hydrolysis using different buffer at pH 9

Figure 14: Initial rate of HPNPP hydrolysis using BORAX at different pH level

Figure 15: HPNPP hydrolysis rate

List of Schemes

Scheme 1: Original simplified synthetic routes for the preparation of ligands

Scheme 2: Original simplified synthetic routes for the preparation of ligands

Scheme 3: Protection of amine (TACN) mechanism using Boc_2O (A), Substitution reaction between diBoc TACN and 5-chloropentyne (B)

Scheme 4: Proposed synthetic route in synthesizing $-(\text{N},\text{N}'\text{-Bis(tert-butoxycarbonyl)-N''-butylguanidiny})\text{-pent-1-yne}$

Scheme 5: Mechanism of Staudinger reduction reaction

Scheme 6: Model reactions of azide substitution (A) and CuAAC click reaction (B)

Scheme 7: Synthesis of Azide-derivatised Merrifield resin (azidomethyl polystyrene) (top route) and Synthesis of model click-derivatised Merrifield resin.

Scheme 8: Synthtic route of “click reaction” of Ligands onto Merrifield resin (Step 1) and deprotection of the Boc protecting groups (Step 2).

Scheme 9: Mechanisms of deprotection of Boc protecting group (A) and formation of 2-methylprop-1-ene (B).

Scheme 10: Three different synthetic route in synthesizing $6\text{-(N},\text{N}'\text{-Bis(tert-butoxycarbonyl)-N''-butylguanidiny})\text{-hex-1-yne}$

Scheme 11: Tosylation mechanism

Scheme 12: Mechanism of Gabriel Synthesis

Scheme 13: Proposed synthetic pathway for pre-immobilized halides. An alternative way to produce immobilized ligands.

List of Tables

Table 1: Solvents, temperature, and time utilised in the synthetic routes illustrated in scheme 10; yield % obtained.

Attestation of Authorship

I hereby affirm that this dissertation is entirely composed of my original work and does not include any content borrowed from other individuals, published articles, or books without proper citation. To the best of my knowledge, I have diligently and independently authored this dissertation.

Marc Agujar Malingin

16th of September

Acknowledgement

I extend my appreciation to my supervisor, Dr. Jack Chen, for his support, guidance, and patience during the course of this project. Dr. Chen provided invaluable insights within the laboratory and sharing his skills and knowledge whenever the opportunity presents. Whenever I faced challenges or sought advice, he was readily available, offering solutions without hesitation. His constant presence made me feel supported throughout this journey, and I never felt alone in my endeavours.

I would also like to express my gratitude to my fellow members in the Chemistry research lab. I extend my sincere thanks to Mohinder for his unwavering support and willingness to assist with any questions I encountered in the lab. His prompt responses and immediate solutions were greatly appreciated. Thank you for making sure that I have everything I need in order to complete this project. This project would not be possible without him. I am thankful to Keer for her companionship, guidance, and for her invaluable assistance in analysing the UV data. Her presence and collaboration were instrumental in the success of this project.

I would like to express my heartfelt gratitude to my family for their love, boundless support, and continuous encouragement. Their unwavering commitment and assistance have been a constant source of comfort and strength throughout my journey. Without their support, I would not have embarked on this academic endeavor, and their presence has been a reassuring balm during the challenges of my Honours program.

In addition, I extend my thanks to my friends for their warm friendship and the comforting atmosphere they provided during this year. Their companionship and the solace of their presence helped me navigate the difficulties and challenges that I have encountered during my studies.

Marc Agujar Malingin

16th of September 2023

CHAPTER ONE: INTRODUCTION

Catalysis stands as an indispensable tool in chemical processes, offering unparalleled benefits such as increased efficiency, energy savings, and waste reduction¹. Specifically, the catalytic performance is closely linked to the composition of the catalyst and the conditions used in experiments². The reaction catalyzed follows an alternative reaction pathway that demands a lower activation energy compared to the original pathway, while the overall free energy of the initial substances and end products remains unchanged. Consequently, catalyzed reactions can be executed more efficiently and with reduced energy requirements. This holds great significance in contemporary society because catalysts play a crucial role in diminishing the energy input for industrial processes and contribute to a reduction in waste production.

This dissertation will revolve around one main objective. We aim synthesize an immobilized catalyst on a resin and demonstrate their "cooperativity." Throughout this dissertation, "cooperativity" refers to the capacity of one or multiple functional groups to collaborate in accelerating a chemical reaction. This phenomenon is a common characteristic of enzymes, the natural catalysts in our bodies that expedite chemical reactions essential for our survival. Nature's enzymes surpass the efficiency of synthetic catalysts we can create, sparking a growing interest in developing synthetic catalysts that emulate their natural counterparts. This dissertation will explore the potential advantages of employing cooperative catalysis within synthetic systems and optimizing the synthetic route to give the most efficient steps into obtaining the desired compounds.

1.1 Bioinspired catalysis

Enzymes represent highly remarkable biological catalysts that possess the extraordinary capability to accelerate chemical reactions by up to 10^{19} times for specific substrates and reactions³. Without enzymes, essential life processes both within and outside cells would be impossible, as the fundamental chemical reactions required cannot occur without catalysis. Enzymes play a vital role in virtually all critical life-sustaining physiological functions, including food digestion, nutrient processing, energy conversion, detoxification, metabolic waste transformation, growth, tissue regeneration, and healing^{4,5}. Their indispensable role in life processes is evident in their presence in various everyday commercial products like laundry detergents and contact lens cleaning solutions^{6,7}. Additionally, enzymes are employed in the production of alcoholic beverages and dairy products. Furthermore, enzymes have gained prominence in chemical synthesis due to their eco-friendly characteristics, aligning with the principles of green chemistry, which has garnered considerable attention in the scientific community⁸. However, the applicability of enzymes in chemical processes is constrained by their limited substrate specificity, primarily geared toward hydrolytic reactions involving biomolecules such as carbohydrates and lipids. If chemists could replicate and engineer enzymes for more diverse reactions, this limitation could be overcome, leading to transformative possibilities.

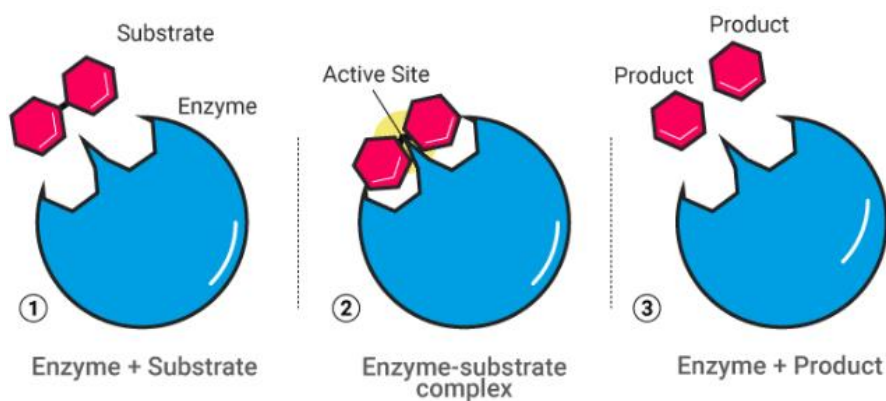


Figure 1: Basic representation of how enzymes catalyze reactions.

Bioinspired catalysis refers to a field of research and technology that draws inspiration from natural biological processes to design and develop catalysts for chemical reactions⁹. As mentioned, catalysts are substances that expedite chemical reactions without undergoing any change themselves during the process. Among all catalysts, enzymes, the catalysts found in biological systems, are exceptionally efficient. Life on Earth, in its diverse forms, relies heavily on enzymes' capacity to accelerate chemical transformations within biochemical processes. Enzymes showcase exceptional vitality, accuracy, and unwavering reliability, emphasizing their deep-seated importance. The pivotal role of enzymes in sustaining life underscores their remarkable effectiveness⁹.

The potential of biomimetic chemistry is unquestionably promising. A comprehensive grasp and application of Nature's catalytic principles offers the possibility of revolutionizing various industries. For instance, by bypassing the need for extreme temperatures and pressures prevalent in modern catalytic processes, truly biomimetic catalysts could facilitate the localized, small-scale production of industrial chemicals. This departure from the traditional economies of scale could lead to significant shifts in chemical feedstock production. As an example, farmers might distribute catalysts on their fields, converting atmospheric nitrogen into ammonia, thus decentralizing the industrial fertilizer production from large-scale facilities to smaller, local processes. Numerous other industries could experience similar transformations by embracing and implementing Nature's catalytic principles⁸. In a seminal 1995 scientific publication featured in the journal *Accounts of Chemical Research*, Ronald Breslow of Columbia University delineated this pursuit as one of the paramount goals in the realm of chemistry, often referred to as a "Holy Grail"^{10a, b, c}. In that publication, he introduced the term "biomimetic chemistry," defining it as "imitating the style of enzyme catalyzed processes in an effort to achieve some of the advantages, which Nature has realized by the use of enzymes"^{10a, b, c}.

In numerous metalloenzymes, transition metals frequently establish coordination bonds with three or four nitrogen atoms, giving rise to metallo-bioactive sites^{11, 12}. Consequently, small polyamino molecules like 1,4,7,10-tetraazacyclododecane (cyclen) or 1,4,7-triazacyclononane (TACN) possess structural attributes that enable them to form highly stable complexes with transition metal ions. Additionally, within metalloenzymes, functional groups are integrated into the catalytic mechanism, often linked to the protein backbone. These groups strengthen the overall interaction with the substrate through mechanisms involving hydrogen bonds, electrostatic contacts, π -stacking, hydrophobic effects, or direct participation in substrate modification processes.

In this specific context, TACN stands out due to its possession of three nitrogen donors, which facilitate the formation of exceptionally stable complexes with transition metals. This property not only prevents the release of metal ions into the solution but also ensures the complex's excellent solubility in aqueous environments. Furthermore, the presence of only three nitrogen donors bound to the metal enhances the metal ions' acidity, leading to the formation of metal-hydroxide bonds. These bonds play a crucial role in various catalytic mechanisms, including the cleavage of phosphate ester bonds or ester bonds. TACN has frequently been employed as a metal-binding site, enabling the creation of mono-, bi-, and polynuclear molecular complexes. Additionally, it has been instrumental in the development of functional nanostructured devices designed for the efficient cleavage of DNA, RNA, or their structural analogues^{13, 14, 15}.

1.2 Benefits of modular assembled catalysis

Enzyme structures are susceptible to disruption due to various environmental factors like temperature, pH, solvent properties, and catalytic concentration. These factors impose practical limitations on the application of enzyme¹⁶. Artificial enzymes have emerged as a promising solution to overcome these operational constraints. Considering these aspects, numerous strategies have been explored to create active sites in enzymes, aiming to establish multiple interactions with bound substrates. One approach involves employing covalent linkers to connect essential functional groups or immobilizing them within molecular frameworks or polymers^{17,18}. Alternatively, functional groups can be attached to complex structures such as dendrimers or nanoparticles. For example, the term "nanozyme" was introduced by Manea and their team in 2004. They illustrated that nanoscale gold particles, modified with thiol compounds containing Zn²⁺ ions, could demonstrate catalytic abilities for phosphate ester cleavage. Nevertheless, artificial enzymes continue to display lower catalytic efficiency when compared to natural enzymes. Therefore, the primary objective for many researchers in recent years has been to enhance catalytic efficiency.

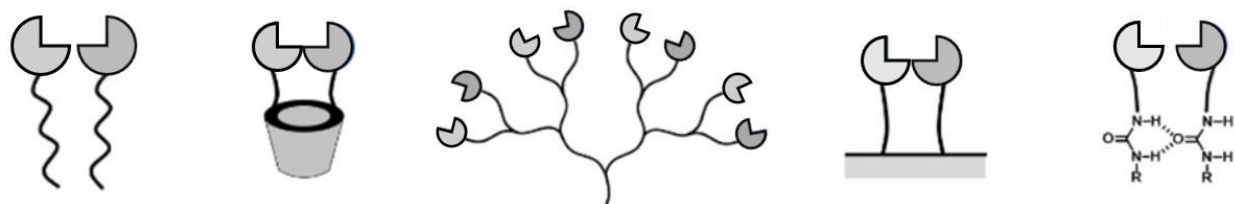


Figure 2: *Different strategies for increasing the activity of cooperative catalysts (left to right; hydrophobic interactions, molecular scaffold, dendrimers, attachment onto surface, hydrogen bonding)*

Modular assemble catalysts offer a valuable platform for the design and optimization of catalysts across a diverse spectrum of chemical reactions. They provide researchers with enhanced control over catalytic processes, leading to improved efficiency and selectivity. These catalysts find applications in various fields, contributing to innovation and sustainability in chemical processes. Modular assembled catalysts offer a flexible and potent method for catalysis, granting the capacity to tailor and enhance catalysts to suit diverse applications, resulting in enhanced reaction rates, selectivity, and eco-friendliness in chemical processes ¹⁷.

1.3 System of interest

In living organisms, enzymes serve as the natural catalysts responsible for facilitating the essential chemical reactions required to sustain life. These biological catalysts have demonstrated remarkable efficiency, surpassing the capabilities of synthetic catalysts developed by chemists. This distinction has motivated chemists to seek inspiration from nature's enzymatic processes. One key factor contributing to the superior efficiency of biological enzymes lies in their ability to employ multiple catalytic groups that function in close proximity and cooperatively interact (figure 3C). This cooperative action enables the simultaneous activation of the starting materials involved in the reactions. This cooperative behavior, known as cooperativity, is the driving force behind the exceptional catalytic rates exhibited by enzymes in comparison to synthetic catalysts, which primarily rely on unimolecular activation mechanisms (figure 3B).

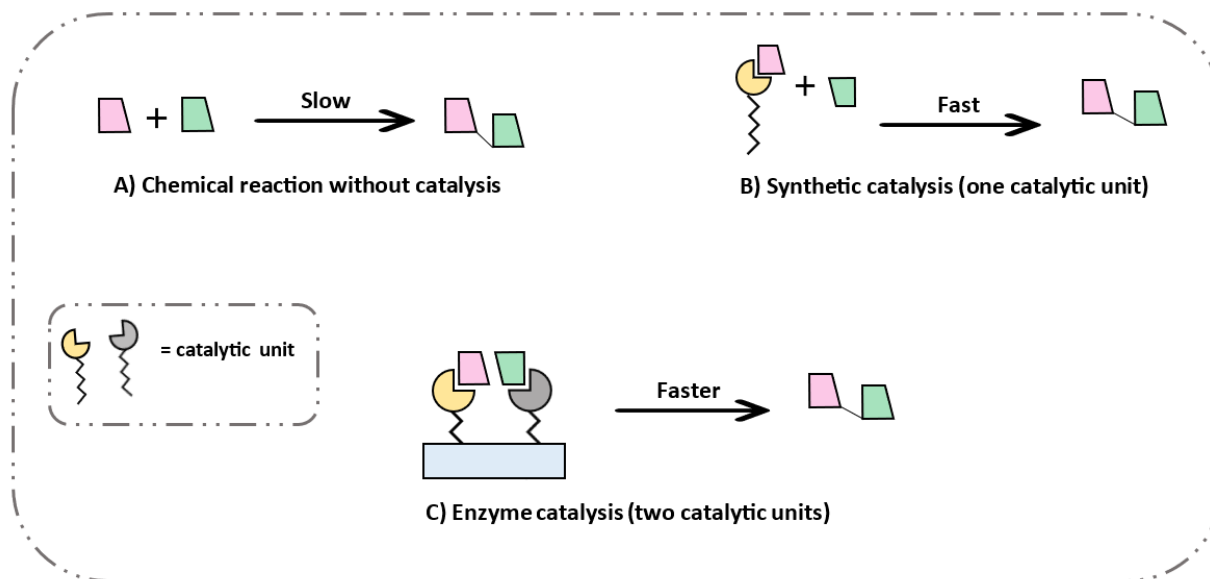


Figure 3: Examples of different catalysis models

In recent times, researchers have made efforts to mimic the cooperative behavior observed in natural systems within synthetic catalysts to enhance their effectiveness. As briefly touched on, in 2004, Manea and colleagues introduced a transphosphorylation catalyst based on gold nanoparticles. This synthetic catalyst exhibited several characteristics reminiscent of natural enzymes, such as cooperativity and saturation kinetics (refer to Figure 4)¹⁹.

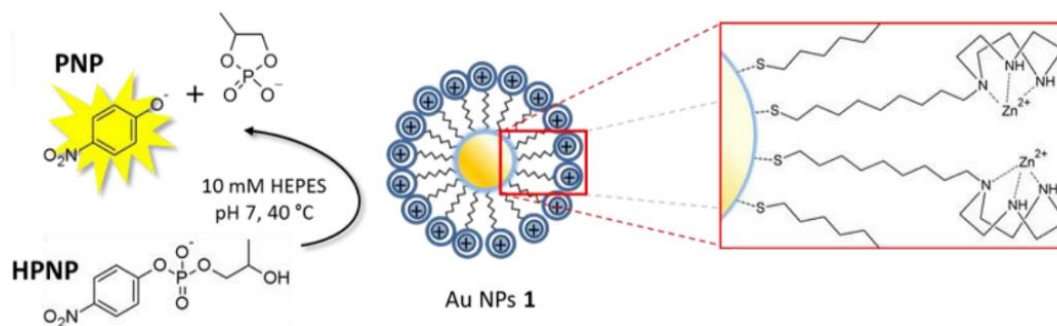


Figure 4: Nanozymes created by Manea and co-workers ¹⁹.

Manea's system involved the incorporation of TACN ligands onto the surface of gold nanoparticles, achieved through the use of thiol functional groups for attachment. This physical bonding of TACN ligands to the gold nanoparticle surface enforced their close proximity. These TACN ligands possess a strong affinity for binding zinc ions, effectively bringing them into immediate proximity for the cleavage of 2-hydroxypropyl p-nitrophenyl phosphate (HPNP), a model substrate used for RNA cleavage studies. In previous research conducted within our group, we successfully developed an artificial system that induced the formation of vesicle-like structures through self-assembly, resulting in the creation of highly efficient catalytic pockets. This system featured an amphiphilic compound named C₁₆-TACN-Zn²⁺, which included a Zn²⁺-complexed 1,4,7-triazacyclononane head group. This compound demonstrated its effectiveness as a catalyst for the cleavage of phosphodiester bonds²⁰.

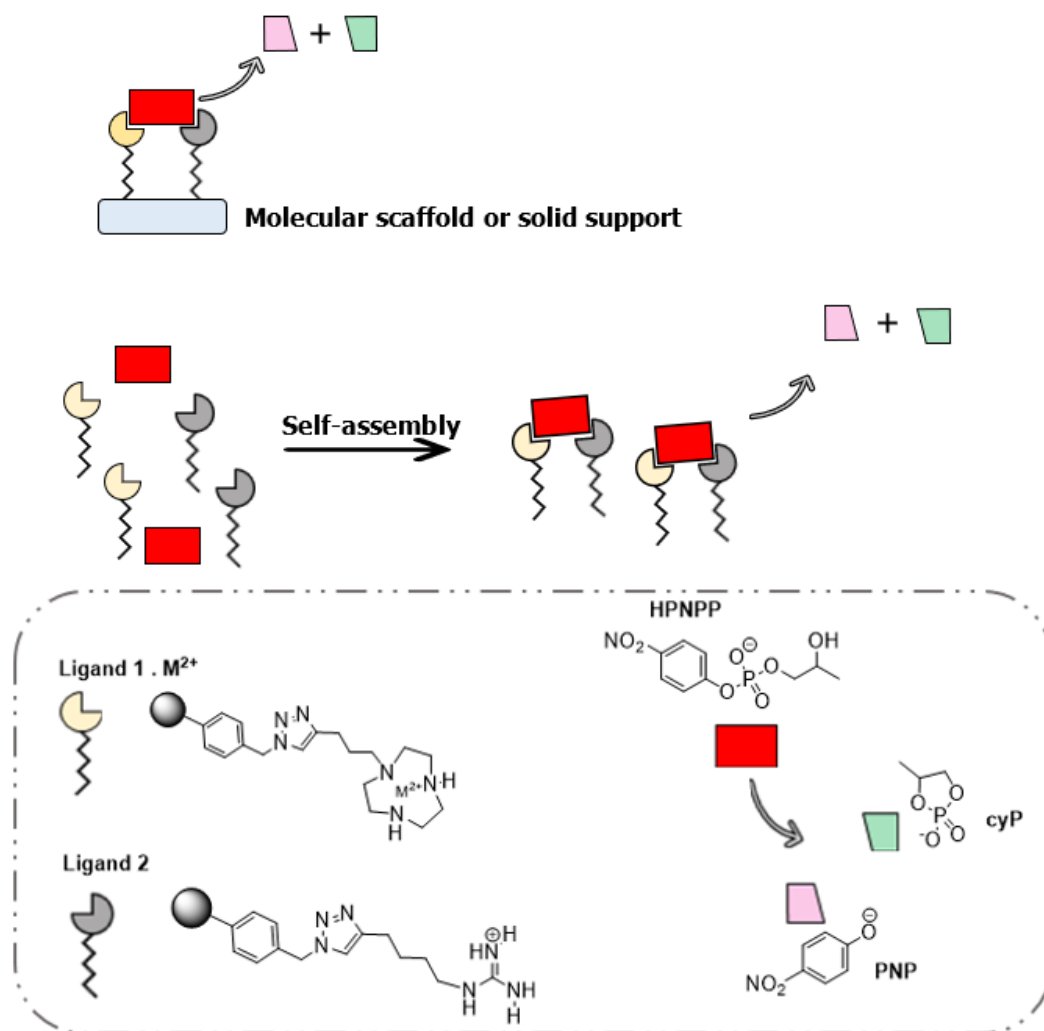


Figure 5: Cooperative artificial catalyst system demonstrating covalently-bound system (top) and self-assembly (bottom).

Furthermore, in addition to the TACN ligand, another artificial catalytic component explored in this system was the guanidinium unit, which is recognized for its cooperative action²¹. The guanidinium group, similar to the amino acid arginine found in many enzymes' active sites, is known for its strong interaction with phosphates through a two-point hydrogen bonding motif²². Synthetic phosphodiesterases have been designed to exhibit cooperativity between guanidinium units and metal-bound ligands. It is believed that the guanidinium unit complements the catalytic function of metal ions by facilitating substrate binding and activation, along with the stabilization of the transition state²³.

To replicate the close proximity observed in natural catalytic enzymes and Manea's gold particle system, we drew inspiration from the idea of anchoring these ligands onto a solid-phase support, specifically Merrifield resin, utilizing copper-catalyzed azide-alkyne cycloaddition, often referred to as "click chemistry." Dr. Robert L. Merrifield, an esteemed American biochemist, is credited with the discovery and pioneering of Merrifield resin. His groundbreaking work in the realm of solid-phase peptide synthesis using resin supports was honored with the Nobel Prize in Chemistry in 1984. Solid-phase synthesis, a versatile and potent method in chemical synthesis, involves conducting chemical reactions on a solid support, in contrast to traditional solution-phase reactions ²⁴.

The solid support usually consists of beads made up of polymers such as, polystyrene, which was the first example invented by Dr Merrifield, polyamide, which is good for polar products, and 80% polyethylene glycol cross-linked to polystyrene, which gives the environment similar to ether or THF. Before the reaction takes place, the beads need to first be left with solvent to "swell". The swelling allows the access of reagents and solvents in order to proceed to react (figure 6A). These resins are functionalized with a chemical reactive attachment point called the "linker". The Merrifield resin used in this project is the original, Merrifield resin, which contains a chloro-methyl group as a linker. This is beneficial for attachment of nucleophiles as it can easily undergo nucleophilic substitution and displace the chloride. Various resin types are illustrated in Figure 6C, each characterized by specific linkages. These linkers are selected to align with the intended attachment of the starting material and the release of the chosen functional group upon completion of the synthesis.

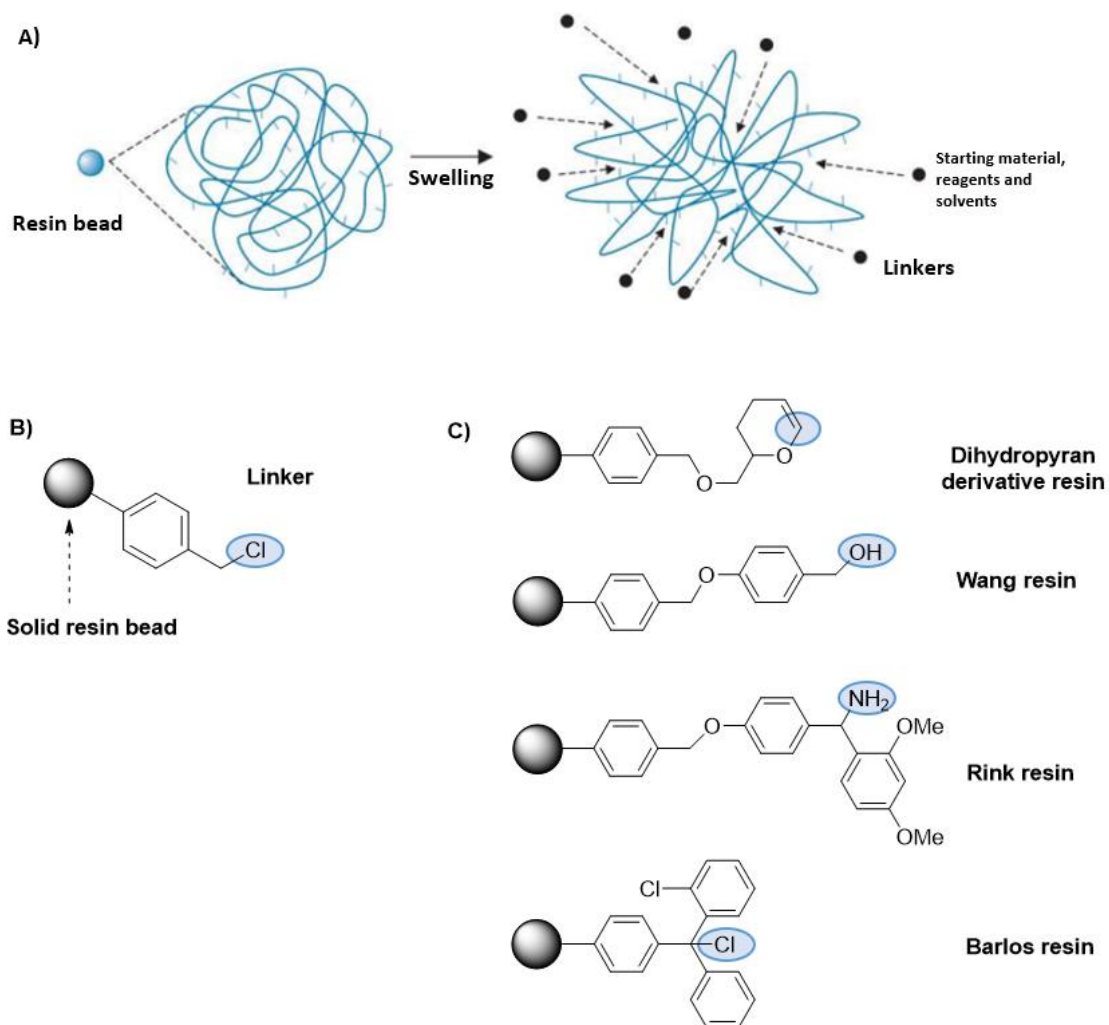


Figure 6: Swelling of resins to allow access of solvent and reagents (A), representation of the parts of the resin (B), examples of different types of resins (C).

This approach has achieved significant recognition within the fields of organic chemistry, biochemistry, and medicinal chemistry due to its numerous advantages, including enhanced purity, efficiency, automation capabilities, recyclability, parallel synthesis, and environmental friendliness, among others. The high surface area of the resins due to their porous and bead-like structure facilitates efficient chemical reactions and the binding of molecules to themselves²⁴. In solid-phase synthesis, a chemically reactive group is affixed to a solid support, facilitating sequential chemical reactions through the addition of reagents. After each reaction

step, unreacted reagents are removed through washing, leaving the desired product firmly attached to the solid support. This methodology enables the efficient isolation and purification of the final compound.

As previously mentioned, the ligands were affixed to these resins with the aim of catalyzing the transphosphorylation of 2-hydroxypropyl p-nitrophenyl phosphate (HPNP), a model reaction employed to simulate RNA cleavage (figure 7). The cleavage of phosphate bonds within phosphodiesterases necessitates cooperativity involving a minimum of two metal ions derived from the active sites of enzymes operating synergistically. Fortunately, the reaction rates can be conveniently monitored using a spectrophotometer. This is facilitated by the release of p-nitrophenolate (PNP) upon the hydrolysis of HPNP, which can be spectrophotometrically tracked at 405 nm. Given that this model reaction is highly pH-dependent, a variety of different buffers were employed and examined during the preliminary investigations.

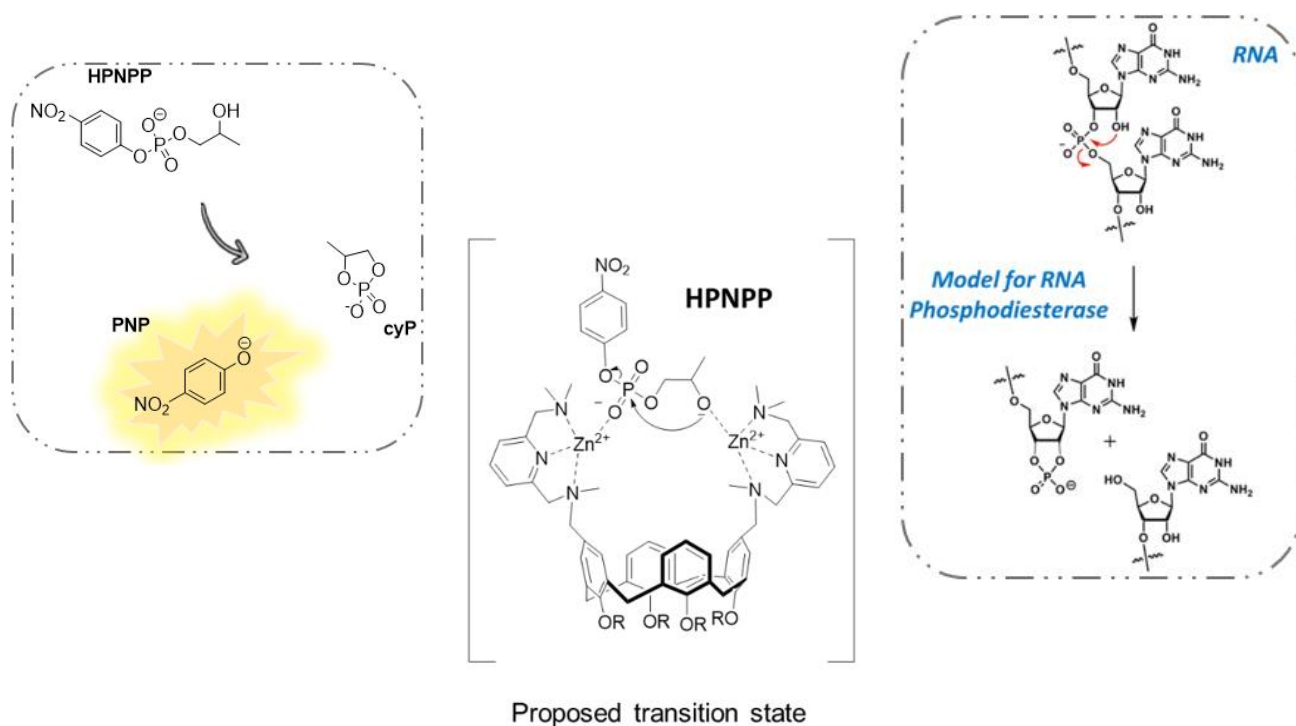


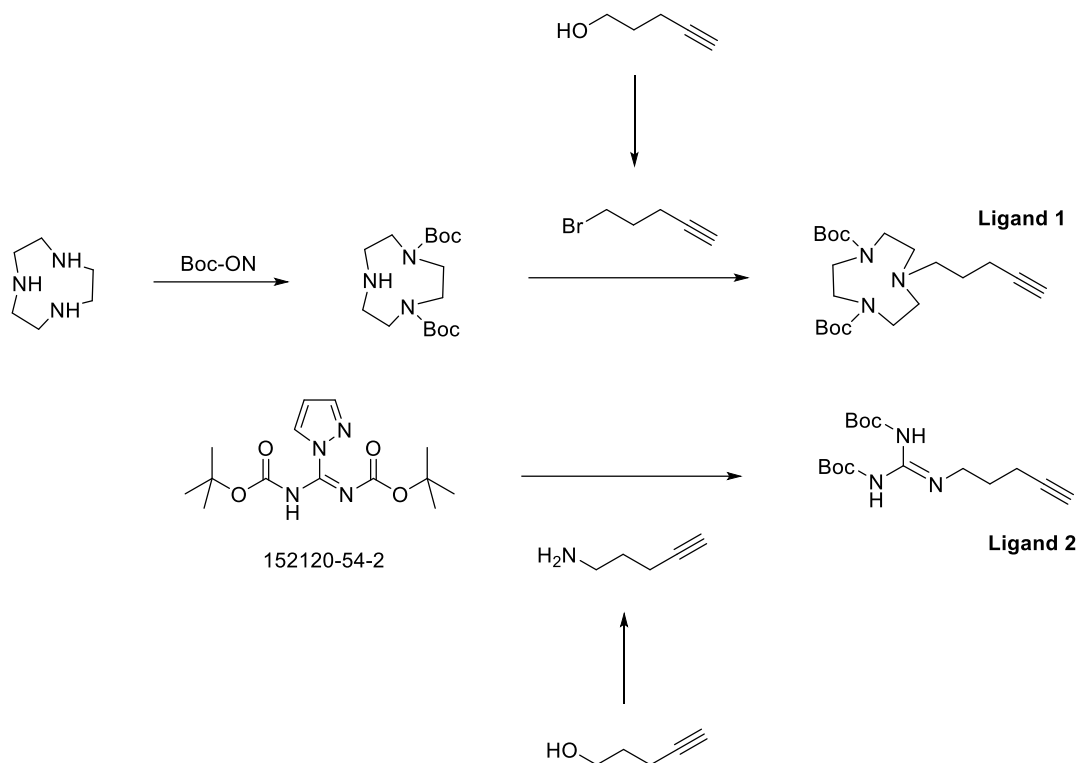
Figure 7: Hydrolysis of HPNPP and proposed transition state, used an RNA cleavage model.

The exploration of synthetic catalysts designed to emulate natural systems extends beyond the potential for enhanced reaction acceleration. Synthetic systems generally exhibit a lower degree of complexity compared to biological enzymes, affording greater flexibility in optimization by chemists. Additionally, the incorporation of supplementary functionalities, such as responsiveness to external stimuli, becomes achievable with synthetic catalysts. This adaptability empowers chemists to refine catalysts more effectively and usher in a new era of intelligent materials and smart catalysts, capable of controlled catalytic activity. Ultimately, the development of increasingly efficient catalysts holds the promise of waste reduction, reduced energy consumption, and enhanced sustainability within industrial processes.

In this research, we are merging our understanding of cooperativity catalysis involving ligand A with itself and ligand B with itself and immobilizing these key functional groups onto a solid resin. From this, two key advantages can be obtained: firstly, the ability to incorporate different types of ligands to optimize its ability to catalyze a reaction. Secondly, the catalysts will be immobilized onto a solid resin, which makes them recoverable and reusable. This is only one of the major advantages over catalysts previously synthesized with the group²⁰. It is essential to note that these catalysts will not be solubilized within a traditional "solution." Instead, they will be suspended in a chosen solvent, and this heterogeneous nature will allow the immobilized artificial catalysts to be easily separated from the solution and be reused.

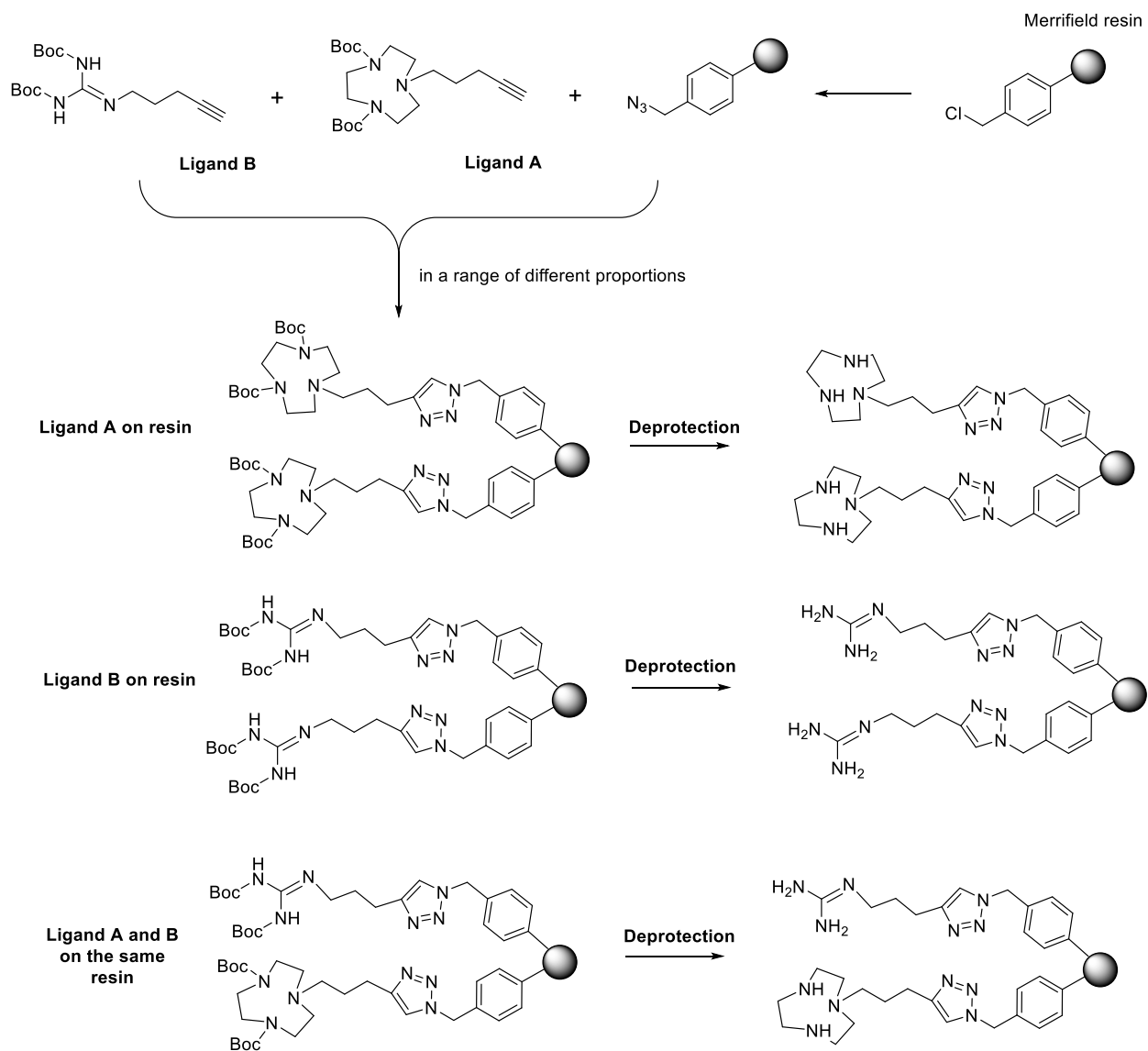
1.4 Aim of the research

The primary aim of this study is to create an immobilized transphosphorylation catalyst inspired by enzymes. To achieve this aim, several key objectives have been outlined. Foremost among them is the synthesis of both TACN (A) and guanidinium (B) ligands. The original simplified synthetic routes for the preparation of these ligands are illustrated in the figure below (scheme 1).



Scheme 1: Original simplified synthetic routes for the preparation of ligands

The following objective is to immobilize these ligands onto resin and establish a bioactive site. This procedure entails the use of a copper-catalyzed azide-alkyne cycloaddition (CuAAC) "click reaction." The original and simplified synthetic pathways for accomplishing this are established in scheme 2 below. These routes are specified and optimized to address issues related to volatility, enhance the percentage yield, and streamline the overall process. Detailed discussions of these optimization processes will be presented in the following chapter.



Scheme 2: Original simplified synthetic routes for the preparation of ligands

Lastly, the final objective was to assess the catalytic activity of these supported catalysts employing the model substrate HPNPP. This aimed to determine the ideal conditions for catalytic activation and to illustrate the presence of cooperativity in the catalytic process.

CHAPTER TWO: RESULTS AND DISCUSSION

2.0 Overview

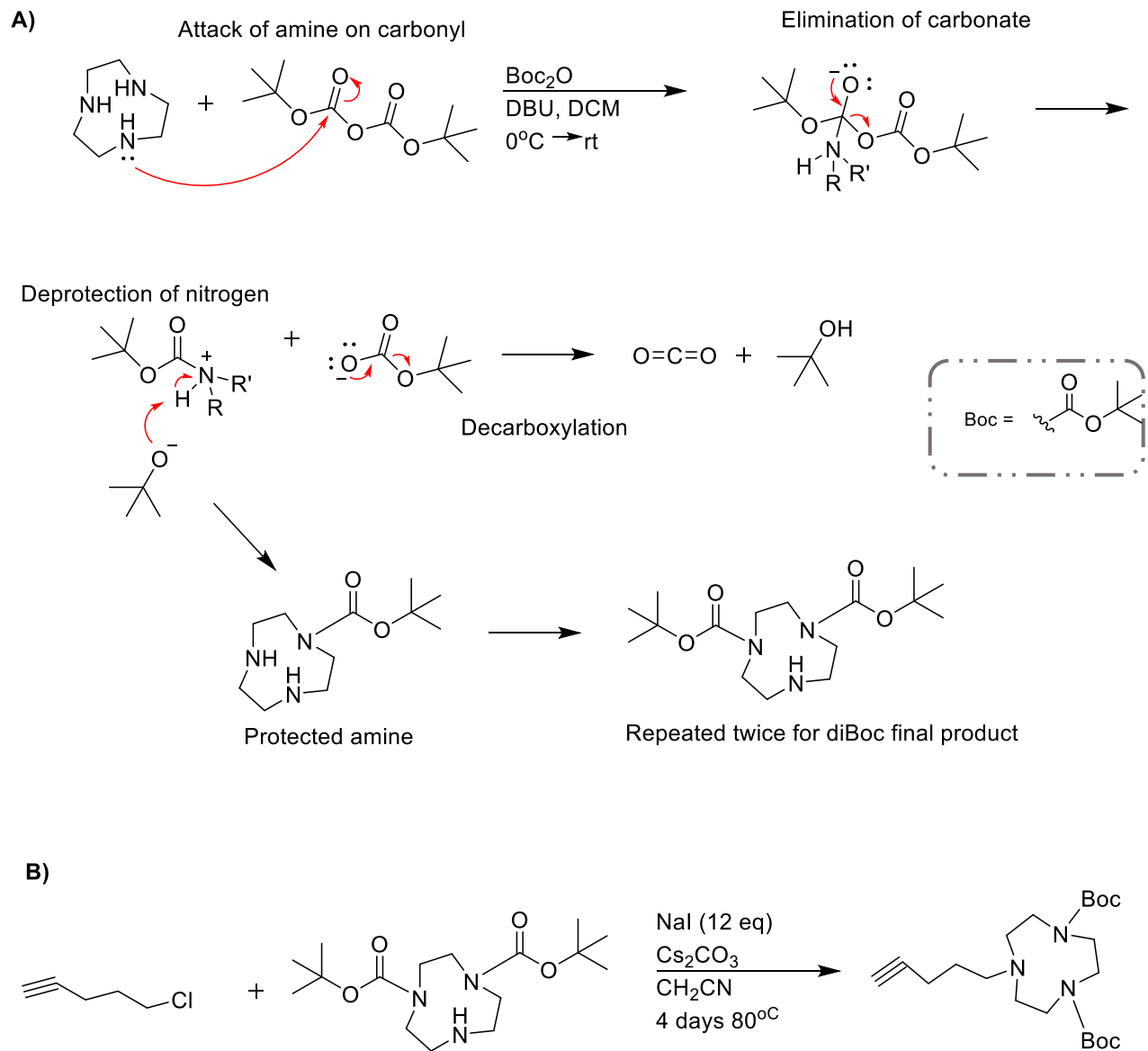
The primary objective of this study was to create and synthesize an artificial enzyme with the necessary attributes for immobilized cooperative catalysis. Molecules were designed to incorporate ligand head groups capable of catalytic activity, along with a reactive tail group that could be easily linked to the resin support material. The ligands selected for this purpose were C₅-TACN and (1^b) C₆-guanadinium (2^b). Previous research conducted within our research group had demonstrated the efficient catalytic properties of the Zn²⁺-complexed TACN head group and guanidinium head group, respectively, particularly in the cleavage of HPNPP. Both of these ligand chains were designed to include an alkyne group at their tails, facilitating their attachment to the resin support, which, in turn, featured an azide group for this purpose, utilizing a "click" reaction. The comprehensive design details for these ligands, along with the desired molecular structures will be addressed in later sections.

Initially, the "click" reaction was evaluated through preliminary reactions utilizing different azides to assess the efficiency and efficacy of the reaction. For this purpose, Nuclear Magnetic Resonance (NMR) spectroscopy at a frequency of 400 MHz was employed to monitor these reactions. Subsequently, once the reaction conditions were established, they were applied to the resin-bound systems. In these cases, infrared (IR) spectroscopy was utilized to monitor the progress of the reactions and determine their completion. This approach allowed for a comprehensive investigation of the "click" reactions and their application to the resin systems.

Following the optimization of the synthetic pathway and successful attainment of the desired product and route, the study turned its focus to examining the most favorable conditions for the catalysis of HPNPP. The enzymatic activity, specifically the rate of phosphodiesterase action on HPNPP, was assessed using UV-visible spectroscopy at a wavelength of 405 nm. This analysis allowed for a comprehensive investigation into the catalytic performance under various conditions, ultimately leading to valuable insights. The synthetic plan on how to synthesize all the compounds on this project is presented throughout this chapter.

2.1 Synthesis of di-*tert*-Butyl 7-(pent-1-yn-5-yl)-1,4,7-triazacyclononane-1,4-dicarboxylate

The initial phase of this project was to design and synthesis of the primary ligand, C₅-TACN alkyne. The synthesis of this ligand was achieved through a concise two-step process. Initially, the TACN substrate underwent protection with a *tert*-butylcarbonyloxy (Boc) group to ensure that nucleophilic substitution, in the subsequent step, occurred at a single site within the TACN substrate. This protective step involved dissolving TACN.3HCl in dichloromethane within a nitrogen (N₂) environment, followed by the addition of DBU, and subsequent cooling to 0 degrees Celsius. Then, the Boc protective group was gradually introduced to the mixture via a syringe pump to maintain a consistent addition rate and prevent the formation of undesired byproducts, such as TANC tri-Boc. The reaction was allowed to proceed for an additional 4 hours at room temperature to ensure complete reagent conversion. The unreacted reagents were then quenched and neutralized, and the resulting crude product underwent purification through flash column chromatography, yielding compound **1** (scheme 3a). The NMR spectra showed a distinct peak at around 1.36 ppm that integrates for 16 protons, which is the indication of the 2 Boc protecting groups. Attached to the molecule is a distinct single peak at around 1.2 ppm which indicates the alkyne single proton.

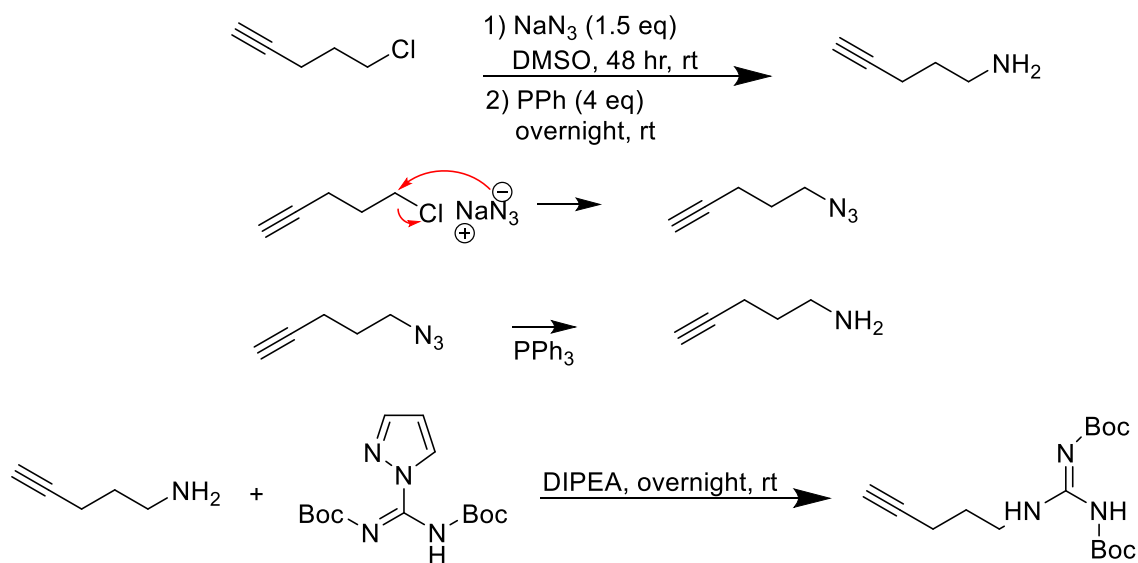


Scheme 3: Protection of amine (TACN) mechanism using Boc_2O (A), Substitution reaction between diBoc TACN and 5-chloropentyne (B)

Following the protective step, an alkylation reaction was conducted by combining 10 eq of 5-chloropentyne with compound **1**. This alkylation reaction was carried out under reflux conditions at 80 degrees Celsius, and the reaction mixture was allowed to react for a duration of 4 days. Upon completion, the reaction mixture underwent filtration through celite, followed by evaporation and purification, resulting in the formation of C₅-TACN alkyne (**2**) with a yield of 75% percent (scheme 3b). The designed di-*tert*-Butyl 7-(pent-1-yn-5-yl)-1,4,7-triazacyclononane-1,4-dicarboxylate was successfully synthesized, and this was confirmed by via NMR.

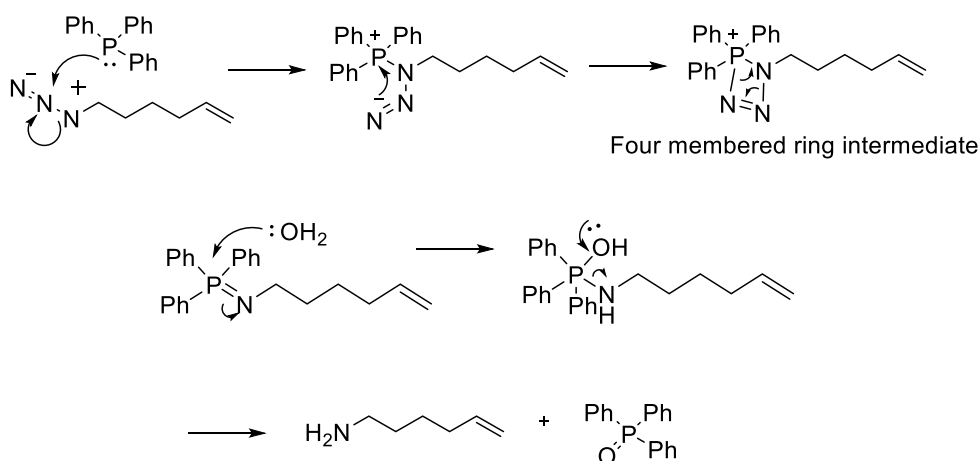
2.2 Synthesis of 5-(*N,N*-Bis(*tert*-butoxycarbonyl)-*N'*-butylguanidinyI)-pent-1-yne

The synthesis of this ligand proved to be a challenge due to the obstacles faced along the way. Before any optimizations, the first synthetic route followed was a very standard procedure. This route is illustrated below on scheme 4.



Scheme 4: Proposed synthetic route in synthesizing 5-(*N,N*-Bis(*tert*-butoxycarbonyl)-*N'*-butylguanidinyI)-pent-1-yne

The same alkyne utilized in the synthesis of the initial ligand was employed in a reaction with 1.5 equivalents of sodium azide, resulting in a substitution reaction. Following the completion of this reaction, 4 equivalents of triphenylphosphine (PPh_3) were introduced into the reaction vessel to further reduce the azide and yield the desired compound. This reaction is commonly known as the "Staudinger reaction" and is recognized for its mild azide reduction properties. The reaction mechanism commences with the interaction between triphenylphosphine (PPh_3) and the azide, resulting in the formation of a phosphor-azide compound. Subsequently, the terminal nitrogen atom establishes a bond with phosphorus, creating a strained four-membered ring intermediate shown in scheme 5. This high strain in the ring promotes the formation of nitrogen gas as a leaving group. The reaction then proceeds as lone pairs of oxygen attack the phosphorus, causing electron redistribution and the cleavage of the double bond between phosphorus and nitrogen. A primary amine was thought to be obtained in a quantitative yield, and the reaction did not necessitate further purification through column chromatography since there were no available instruments to confirm the success of the reaction. The crude material was advanced to the subsequent step, assuming a 100% conversion rate.



Scheme 5: Mechanism of Staudinger reduction reaction

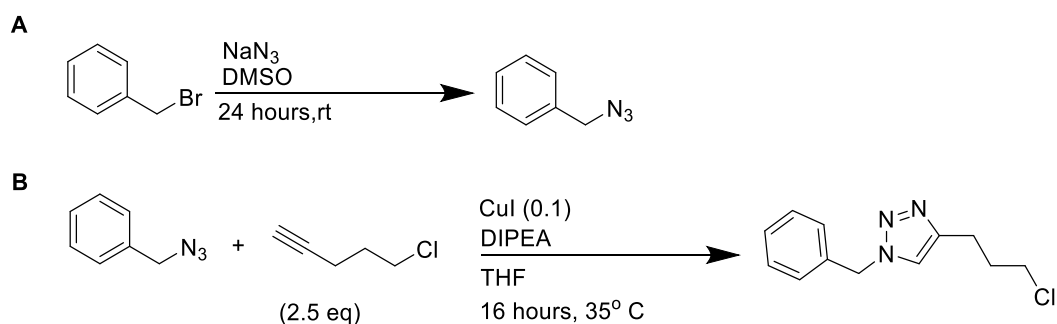
The final stage of this synthesis entails the incorporation of the guanidine functional group by reacting the obtained amine with *N,N'*-Bis-Boc-1-guanylpurazole. Within the guanidinylation reagent, two Boc protective groups are present to protect the nitrogens, ensuring that the nucleophilic substitution reaction exclusively transpires at the intended site. In this reaction, DIPEA serves as both a base to neutralize the reaction mixture and the solvent for the reaction.

Without any confirmation again, it was assumed that the desired had been successfully isolated, and the reaction proceeded to the next step, which involved immobilization.

2.3.0 Synthesis of Immobilized Catalyst

2.3.1 Synthesis of Merrifield resin

The initial step in this reaction involves a substitution reaction wherein the chloride group is substituted with the intended azide group, which will subsequently be employed in the "click" reaction. Following this, the azide compound is reacted with an alkyne to execute the said reaction. To facilitate this, a model reaction was drawn, as illustrated in the scheme below. The rationale behind this approach was to ensure that the reactions progressed to completion under the specified conditions. These reactions were closely monitored using TLC and NMR. It is important that these reactions yield the desired product and are tracked through NMR analysis because once they are on the solid resin beads, NMR monitoring becomes unfeasible.



Scheme 6: Model reactions of azide substitution (A) and CuAAC click reaction (B)

As shown, the initial step involved the reaction of benzyl bromide with sodium azide at room temperature for a duration of 24 hours (scheme 6a). This reaction exhibited great promise as it not only yielded a clean product that required no further purification but also achieved an impressive yield of > 80%. The resulting compound (**10**) was then subjected to a reaction with 5-chloropentyne, addition of DIPEA, THF, and CuI, and left to stir for an additional 16 hours at 35 degrees Celsius while being flushed with nitrogen gas (scheme 6b). Within the flask, white solids and a yellow oil-like liquid were formed. NMR analysis of the yellow oil indicated the formation of the desired product as the triazole group was observed. Furthermore, while the white solid was not subjected to further testing, it was observed that it could dissolve in solvents such as DMSO and MeOH, which is crucial for the future immobilization reactions. This is significant because during the "click reaction" performed on the solid resin, no additional purification steps would be required, as any excess reactants could simply be flushed and filtered using various solvents. Additionally, any impurities present, even if they were in the form of white solids, could be dissolved in DMSO and/or MeOH and filtered, highlighting one of the major advantages of "solid-phase synthesis."

Following these initial reactions, the synthesis was carried out on the Merrifield resin. The schematic representation below illustrates the immobilization of a substitute alkyne chain and once again, the "click reaction" was tested on the resin with a substitute alkyne. To achieve the conversion of the chloride to azide, slight modifications were made to the conditions in comparison to the trial reaction shown in the scheme earlier. Although the same reagent, sodium azide, was employed, the reaction was heated to 60 degrees Celsius to enhance the reaction rate and left to stir for a minimum of two days to yield compound **10**. The Merrifield resin was subjected to a washing procedure involving DMSO, methanol, and dichloromethane to eliminate excess reagents and dissolve any impurities.

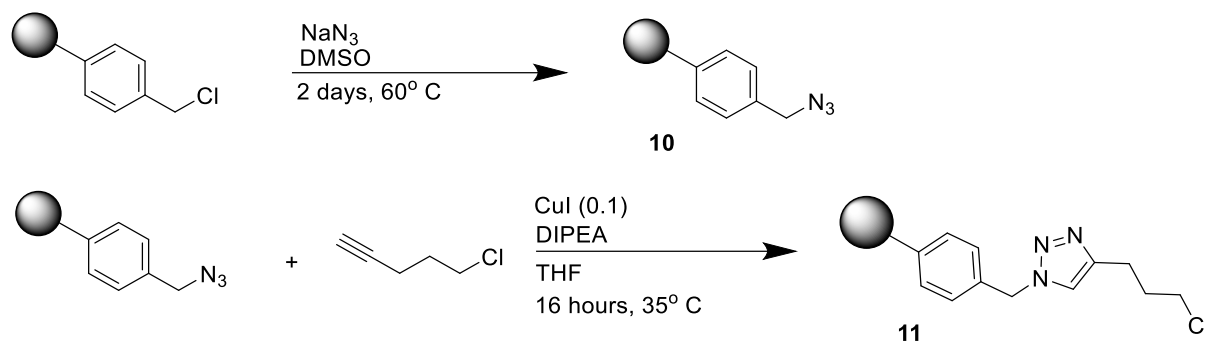
This step was of paramount importance because it revealed distinctive behaviors of the resin when exposed to different solvents. Refer to the images presented below (figure 8), which shows the resin's response to washing with DMSO and MeOH (left), where it appeared to contract noticeably, and to washing with DCM (right), resulting in significant volume expansion or "swelling." This observation holds valuable implications for the utilization of these catalysts in subsequent kinetic studies.



Figure 8: Representation of how the Merrifield resin behaves under MeOH/DMSO (left) and CH_2Cl_2

In order to confirm the formation of the product, infrared spectroscopy (IR) was utilized. The presence of azide was evident from a strong peak at 2093 cm^{-1} . However, a relatively low percentage yield of 43% was obtained, primarily attributed to my limited understanding of the resin's behavior. It was observed that a significant portion of the product was lost during the application of pressure due to the free-flowing nature of the resins. This was noted for subsequent experiments, and measures were taken to prevent resin loss, such as the addition of cotton during high vacuum procedures.

To follow, the "click reaction" was executed on the resin by combining compound **10** with an alternative alkyne, 5-chloropentyne, under the same previously employed conditions. After the reaction concluded within 16 hours, the mixture underwent filtration using a filter funnel, followed by thorough washing with DMSO, MeOH, and DCM, and put under high-pressure to eliminate excess solvents. The resulting product was subject to analysis via IR spectroscopy, revealing the conspicuous absence of the azide peak. This observation strongly indicates that the reaction reached completion, with all azide groups successfully reacting with the alkyne which solidifies the conditions used to be performed on the catalyst substrates.

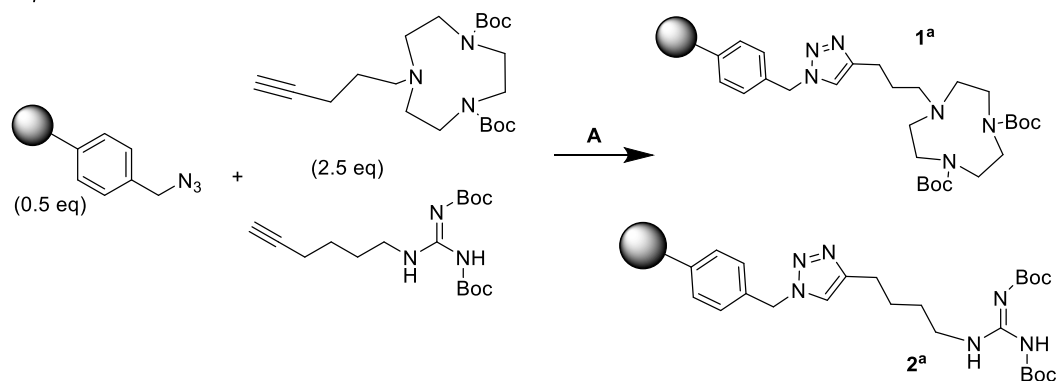


Scheme 7: Synthesis of Azide-derivatised Merrifield resin (azidomethyl polystyrene) (top route) and Synthesis of model click-derivatised Merrifield resin.

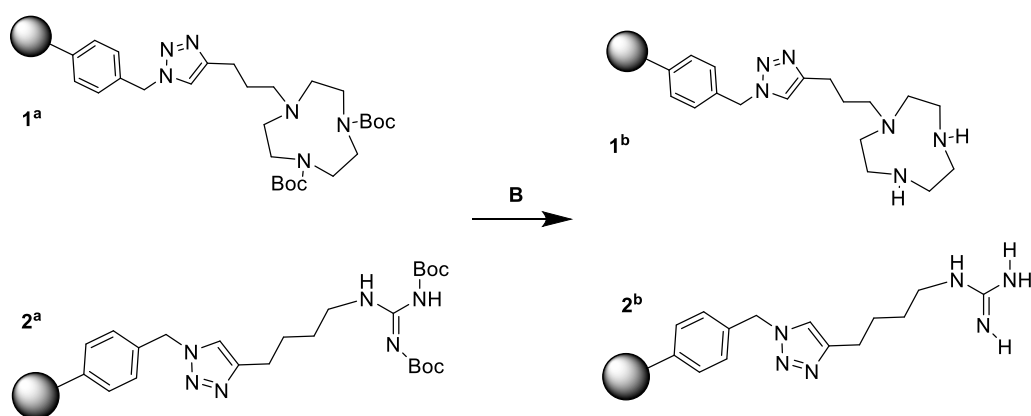
2.3.2 Immobilizing ligands via CuAAC “click reaction.”

The concluding phase of the synthesis process involves the immobilization of the ligands. With well-established and validated conditions for optimal efficiency and efficacy, it was time to execute the "click" reaction to attach the ligands onto the resin. The schematic representation of this reaction plan is provided in scheme 8. Initially, the Merrifield resin that was previously azide-derivatised, was used and reacted with the C₅-TACN alkyne ligand. When the reaction has concluded, this mixture underwent filtration, followed by thorough solvent washing and vacuum drying. Verification of the process involved the examination of product **1^a** using IR spectroscopy, which confirmed the successful formation of the desired product. Notably, the disappearance of the peak at 2093 cm⁻¹ indicated the complete conversion of the azide groups, while the emergence of a peak at 1683 cm⁻¹ signified the presence of the C=O bond associated with the Boc protecting group on the TACN substrate. This observation not only confirmed the reaction's completion but also the formation of the new product.

Step 1: "Click reaction"



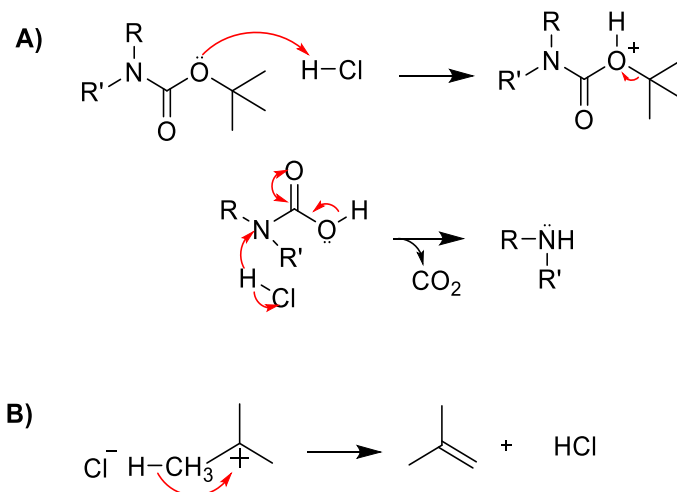
Step 2: Deprotection reaction



Reagents and conditions: **A**) 0.1 equiv CuI, DIPEA, TFH, 4 days, 35 degrees C; **B**) MeOH, 6M HCl, 3 hours, 60 degrees C
 NOTE: Every reaction was washed with DMSO, MeOH, DCM and put under reduced pressure

Scheme 8: Synthetic route of "click reaction" of Ligands onto Merrifield resin (Step 1) and deprotection of the Boc protecting groups (Step 2).

After this phase is the deprotection of the Boc protecting group to yield product **1^b**. This deprotection process was accomplished within a strongly acidic environment, using 6M of HCl. The mechanism of this reaction is illustrated in scheme 9a followed, where the oxygen in the carbonyl group attacks the proton of the hydrochloric acid. Consequently, the *tert*-butyl cation is dissociated due to electron rearrangement, resulting in the formation of 2-methylprop-1-en (scheme 9b). Then, the lone pair of the nitrogen atom accepts a proton, initiating an intramolecular rearrangement leading to the formation of carbon dioxide. Inspection of the IR spectra clearly demonstrates the attainment of the desired product, as evidenced by the disappearance of the stretching peak at 1683 cm^{-1} . This alteration signifies the absence of the C=O group, confirming the successful formation of the desired free amine product, which is now ready for kinetic studies.



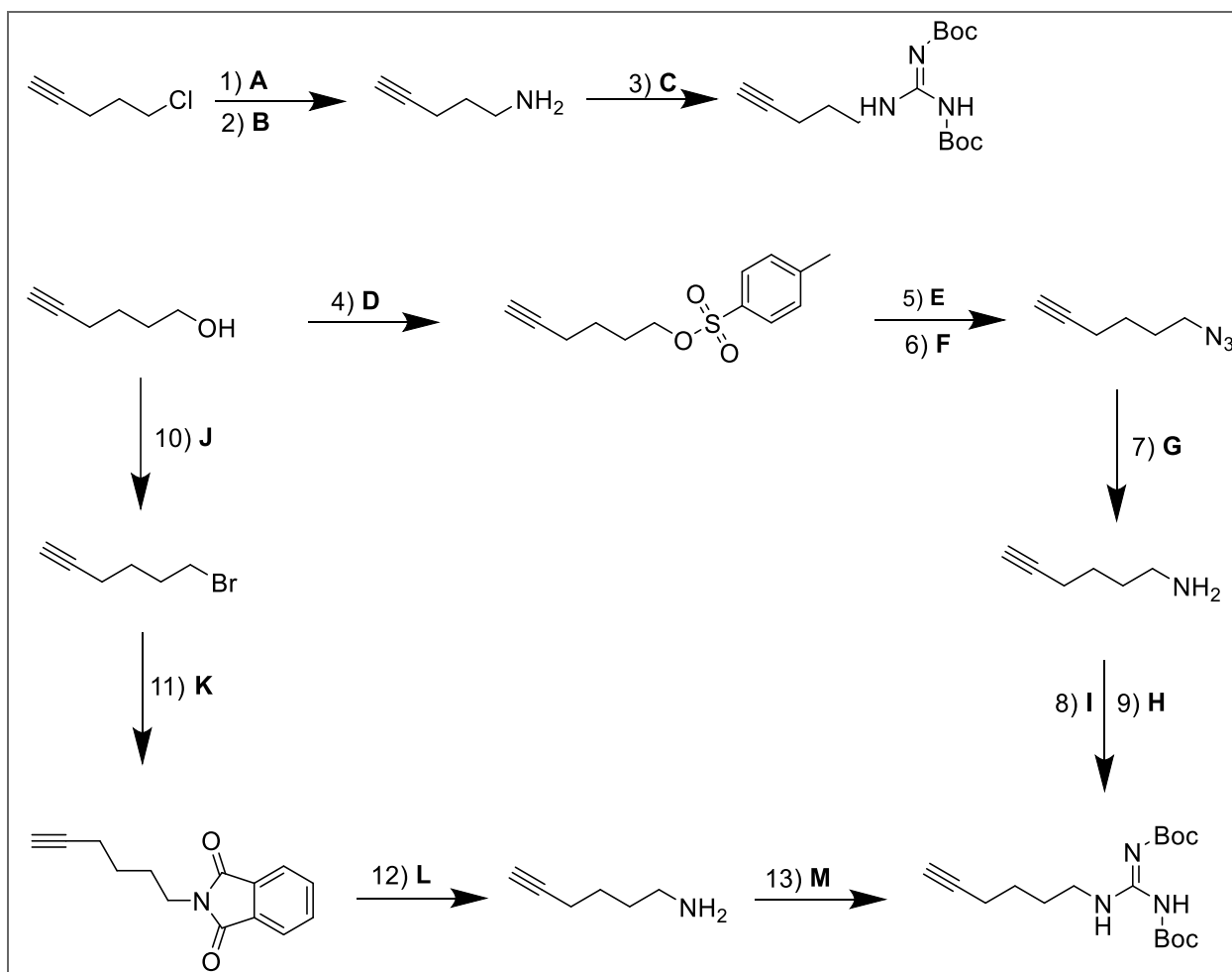
Scheme 9: Mechanisms of deprotection of Boc protecting group (A) and formation of 2-methylprop-1-ene (B).

Moving forward with the immobilization of the guanyl substrate, this was executed utilizing the same procedure applied for the preceding ligand. As previously indicated, there was no confirmation available regarding the synthesis, let alone the purification, of the guanyl substrate. Upon reaction with the Merrifield resin, the established steps and conditions were followed. To confirm the formation of the product, the same analytical tool, IR spectroscopy, was used. Upon examination, it was obvious that the characteristic peak at 2093 cm^{-1} remained, signifying the presence of the azide group on the resin. Importantly, the absence of a peak at 1700 cm^{-1} unfortunately indicated the lack of success in producing **2^a**. A critical consideration at this problem is the necessity for comprehensive characterization of the preceding steps involved in ligand formation prior to proceeding with solid-phase synthesis. Furthermore, it was conjectured that the preceding products might have been volatile, thus impeding their progression to the final stage. Unfortunately, the NMR instrument remained non-operational. Thus, an interim strategy was implemented to optimize an alternative route for the acquisition of **2^b** and is talked about in further detail in the next section.

2.4.0 Optimizations of Synthetic routes

2.4.1 Obtaining Guanidinium substrate.

As previously mentioned, optimizations were necessary to enhance the yield of the C₆-guanyl substrate, improve synthesis efficiency, and address the volatility issue observed in prior compounds. The proposed synthetic route is illustrated in the following scheme. While Route 1 (synthesis steps 1-3) had been established, concerns arose due to the volatility of the intermediate amine and the absence of product confirmations. Therefore, two alternative routes were explored.



Reagents and conditions: **A**) 1.5 equiv NaN₃; **B**) 4 equiv PPh₃; **C**) N,N'-Bis-Boc-1-guanylpyrazole; **D**) TosCl; **E**) 1.5 equiv NaN₃; **F**) 1.5 equiv NaN₃; **G**) PPh₃; **H**) N,N'-Bis-Boc-1-guanylpyrazole; **I**) N,N'-Bis(tert-butoxycarbonyl)-N''-triflylguanidine; **J**) CBr₄, PPh₃; **K**) Potassium phthalimide; **L**) **M**) N,N'-Bis(tert-butoxycarbonyl)-N''-triflylguanidine

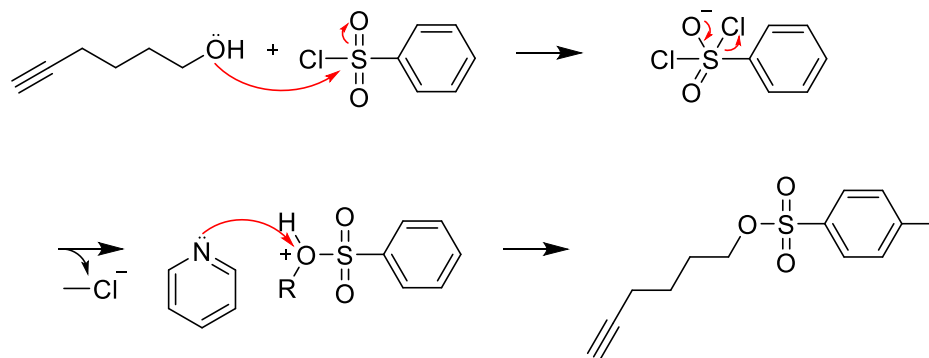
Synthesis no.	Solvent	Temp. (°C)	Time	% Yield
1	DMSO	Rt	48 hours	Estimated 100
2	DMSO	Rt	Overnight	Estimated 100
3	DIPEA	Rt	Overnight	-
4	CHCl ₃	0 → Rt	Overnight	81
5	Acetonitrile	Rt → 80	24 hours	-
6	DMF	Rt	Overnight	43
7	THF/H ₂ O (1:1)	Reflux	Overnight	78
8	DIPEA	Rt	Overnight	39
9	DIPEA	Rt	Overnight	-

10	CHCl ₃	0 → Rt	Overnight	-
11	DMF	90	Overnight	78
12	-	-	-	-
13	DIPEA	Rt	Overnight	

Scheme 10: Three different synthetic route in synthesizing 6-(*N,N'*-Bis(*tert*-butoxycarbonyl)-*N''*-butylguanidinyI)-hex-1-yne

Table 1: Solvents, temperature, and time utilised in the synthetic routes illustrated in scheme 10; yield % obtained.

In Route 2 (synthesis steps 4-8), the starting material was changed from a 5-chain alkyne chloride to a 6-hexyne-1-ol. This modification initiated the reaction by converting the hydroxide into a tosylate compound through a straightforward SN2 nucleic substitution reaction. In this reaction, the oxygen from the alcohol attacked the sulfur atom of *p*-toluenesulfonic acid, forming a bond while displacing the chloride ion. Simultaneously, the chloride ion accepted a proton from the O-H group, ultimately generating HCl gas (scheme 11). The product of this reaction was monitored using ¹H NMR, and the presence of two doublets, each integrating for 2 protons in the aromatic region (7.7 ppm – 7.2 ppm), indicated the formation of the tosylate compound. The concept behind creating a tosylate compound was not solely aimed at generating a more favorable leaving group; rather, it was hoped to potentially increase the boiling point of the alkyne chain, thereby reducing its tendency to undergo vaporization.



Scheme 11: Tosylation mechanism

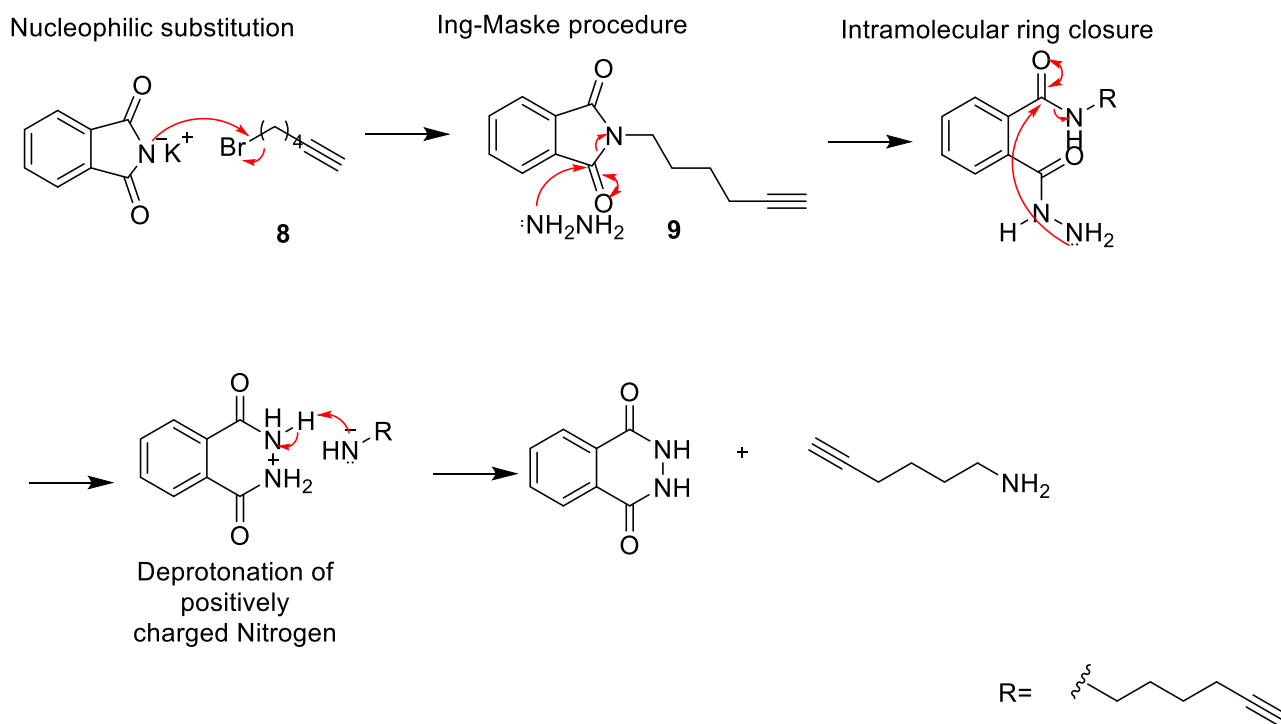
Following this step, the tosylate compound was transformed into an azide compound. The rationale behind using a tosylate as a starting material was to facilitate the conversion into azide, expecting a high yield. In synthesis 5, acetonitrile at room temperature was initially chosen for this synthesis. However, after one day of monitoring the reaction by TLC, it became evident that the reaction was progressing slowly and had not reached completion. The TLC plates showed faint spots where the product should appear and concentrated spots where the starting material was still present. To speed up the reaction, the temperature was increased to 80 °C, and refluxing was employed, allowing the reaction to stir overnight. However, this approach introduced another challenge. During the attempt to isolate the product, it was observed that not only had the solvent evaporated, but the tosylate compound had also evaporated, indicating that the initial rise in temperature caused this unexpected loss. This outcome highlighted the volatile nature of alkynes, especially when they are part of a relatively short carbon chain, such as in this case, a C₆ alkyne. To address these challenges, an alternative solvent, dimethylformamide (DMF), was chosen for synthesis 6. The objective was to maintain the reaction at room temperature to avoid the issues encountered previously. Initially, DMF was not considered due to its high boiling point, which posed challenges for its removal during purification. To mitigate this, ice-cold water was employed to wash the reaction mixture, and dichloromethane was used to facilitate the evaporation of excess DMF. Analysis via ¹H NMR indicated the disappearance of peaks in the aromatic regions and the remainder of other peaks and integrations, signaling the successful formation of the desired product. Although traces of DMF were still present, the progress was sufficient to proceed to the subsequent step giving the highest yield of multiple attempts of <50%.

In the following step, which paralleled route 1, the azide group was efficiently and successfully reduced to a primary amine utilizing the Staudinger reaction (synthesis 7). The process yielded (78%) the desired primary amine product without complications.

The final stage involved the introduction of the guanidine functional group, employing N,N'-Bis-Boc-1-guanylpirazole (synthesis 9). Initially, the same conditions and reagents were applied; however, upon examining the crude product, it became evident that no product had formed, despite multiple attempts at this synthesis. A hypothesis emerged that the reagent N,N'-Bis-Boc-1-guanylpirazole may have deteriorated. As a result, an alternative guanyl reagent, N,N'-Bis(tert-butoxycarbonyl)-N"-triflylguanidine, was employed in synthesis 8. The crude product was obtained and subsequently purified. Analysis via ¹H NMR confirmed the successful formation of this product. The presence of characteristic signals for the two -NH groups and a

very high peak at 1.25 -1.45 ppm that integrated for 18 protons, corresponding to the diBoc group, provided unequivocal evidence for the formation of the product. However, the final yield was again below 50%, falling short of the desired standard, and significant loss occurred throughout the multistep synthesis and volatility of pseudo compounds. This outcome prompted further exploration of an alternative route for the guanyl substrate.

Route 3, the final approach for synthesizing the guanidine substrate, initiated with the same initial compound, a 6-carbon chain alkyne hydroxide. The conversion of the hydroxide to a bromide was achieved through the use of the CBr_4 reagent, a well-established and room-temperature liquid molecule. Furthermore, a planned Gabriel synthesis aimed to convert this alkyl bromide into an amine. The mechanistic aspects of this reaction are drawn in scheme 12. In the initial step, an $\text{S}_\text{N}2$ substitution ensued as the nucleophilic nitrogen of the phthalimide attacked the carbon bonded to the bromine atom, thereby displacing the bromine. Steps yield the alkyl phthalimide, and this was confirmed via proton NMR as there were two sets of doublets evident peaks at the aromatic region. However, it is important to note that due to time constraints, the last two steps of this synthesis were not executed, and consequently, no results were obtained.

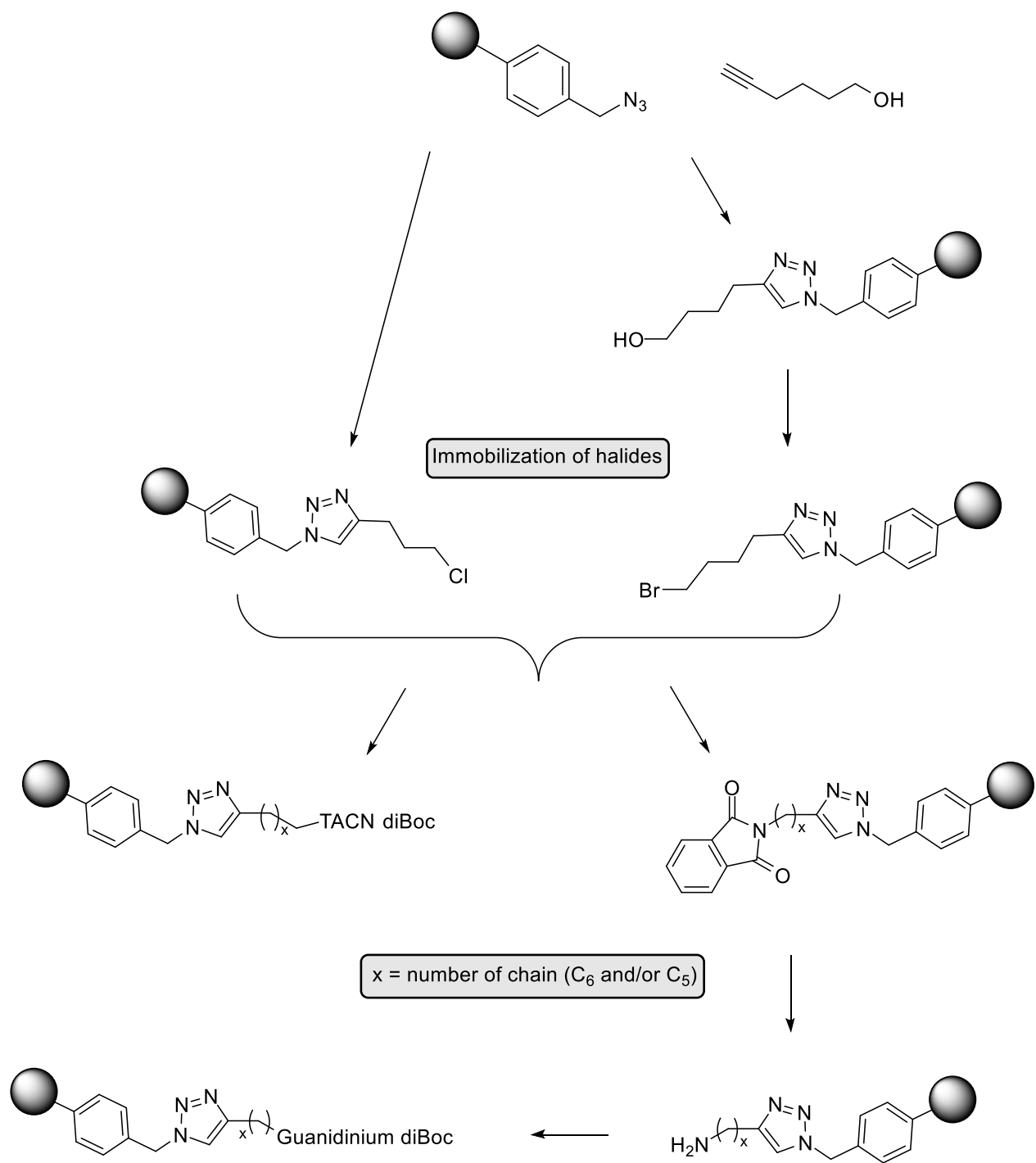


Scheme 12: Mechanism of Gabriel Synthesis

Nonetheless, a detailed mechanistic discussion of these steps is still relevant. The process commenced with a nucleophilic acyl substitution at the carbonyl group, involving the nitrogen atom in the hydrazine. As displayed in Scheme 12, the lone pairs of the nitrogen in hydrazine initiated an attack on the carbonyl carbon, resulting in the cleavage of a 5-membered ring. Subsequently, protonated hydrazine underwent deprotonation through an intermolecular proton transfer facilitated by the negatively charged nitrogen. The next stage involved a second nucleophilic acyl substitution at the carbonyl, facilitated by the unreacted NH_2 of the hydrazine, leading to the liberation of the negatively charged amine. Finally, deprotonation of the positively charged nitrogen by the newly released negative nitrogen led to the formation of the free primary amine and phthalhydrazide. Converting the free amine to 6-(*N,N*-Bis(*tert*-butoxycarbonyl)-*N*'-butylguanidinyloxy)-hex-1-yne would have been the same procedure as previously illustrated in scheme 10. The Gabriel synthesis route proved promising as product 9 yielded just under 80%, but unfortunately was not continued due to time constraints.

2.4.2 Pre-immobilized halides

To address the overall issue of product loss through volatility or multi-step synthesis, an alternative synthetic approach has been thought of. In this approach, an alkyne halide is initially immobilized onto the resin, prior to embarking on the multi-step synthesis. This strategic modification serves to mitigate product loss caused by evaporation, purification, and unreacted starting material. Given the establishment of these synthetic routes, the implementation of this concept is both logical and practical. The proposed synthetic pathway is illustrated as follows.



Scheme 13: Proposed synthetic pathway for pre-immobilized halides. An alternative way to produce immobilized ligands.

As displayed, the proposed approach closely mirrors the original pathway where ligands are synthesized independently before their attachment to the solid resin. The key distinction lies in the immediate "click" immobilization of the starting alkyne halide onto the resin before proceeding further with multi-step synthesis. This initial immobilization of halides onto the resin sets the stage for near 100% conversion in subsequent reactions. Tracking any remaining starting material can be efficiently accomplished through IR spectroscopy if peaks are prominent. Moreover, the unreacted resins can be readily subjected to repeated reactions until 100% conversion is achieved, eliminating concerns about excess and waste of starting material.

Reactions post-"click" can be reasonably assumed to be substantially pure, negating the need for further purification steps. In the event of impurities, liquid impurities can be conveniently filtered, while solid impurities can be dissolved in solvents and filtered. An important consideration is the inability to monitor the purity of reactions post-"click" using NMR spectroscopy. However, given the well-established nature of the proposed synthetic pathway, its reliability is expected.

Another potential concern is the potential exposure of resins to harsh conditions following immobilization, which could potentially damage the resin. However, it is understood that the proposed synthetic route does not involve severe conditions; in fact, the majority of reactions are conducted at room temperature. To validate the viability of this proposal, experimental testing was conducted, and the progress of reactions was monitored using IR spectroscopy.

The spectra presented in the diagram (figure 9) serves as promising evidence not only of the reaction's success but also of the complete reaction of the azide linker within the Merrifield resin. Specifically, the azide-derivatized resin (red) exhibits a prominent peak at 2090.47 cm^{-1} , indicative of the presence of the azide functional group. In contrast, when examining the product (green), there is an absence of any discernible azide-related features, signifying a successful transformation. Furthermore, a broad peak at 3300 cm^{-1} is observed, corresponding to the O-H stretching vibration characteristic of the alcohol moiety.

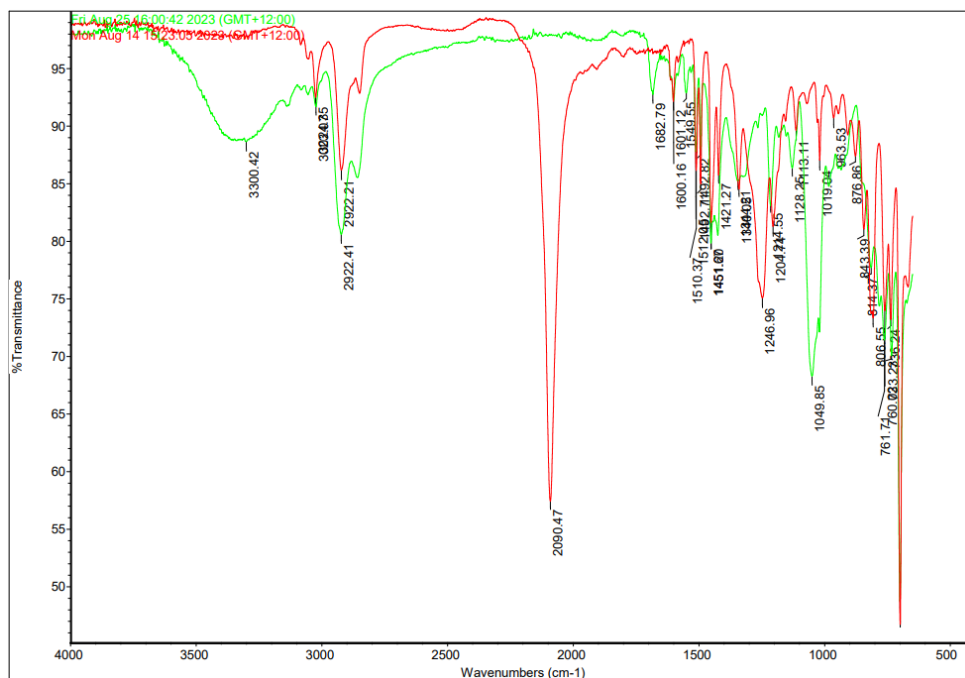


Figure 9: IR spectra of Azide-derivatised resin (red) and post-“click” hydroxy-derivatised resin (green)

A more detailed investigation of this compound was undertaken. The next step in the synthesis pathway involved converting this compound into a halide, achieved by subjecting the resin to a reaction with PPh_3 , CBr_4 , and DCM as the solvent. Figure 10 provides insight into the weakness within this route. Evaluating the spectral data, it becomes apparent that some unreacted O-H linkers remain present in the obtained product (red). However, it is understood that a significant portion of these linkers has undergone reaction, as evidenced by the reduced of the peak at 3350 cm^{-1} in comparison to the starting material (pink). Additionally, a noticeable broad peak at 2456 cm^{-1} is observed, which may potentially indicate the presence of an impurity. Unfortunately, due to the limitations in NMR analysis for resin-based materials, it is impossible to definitively identify or confirm the nature of this impurity, if indeed it is one. This particular aspect highlights a significant drawback within this synthetic route.

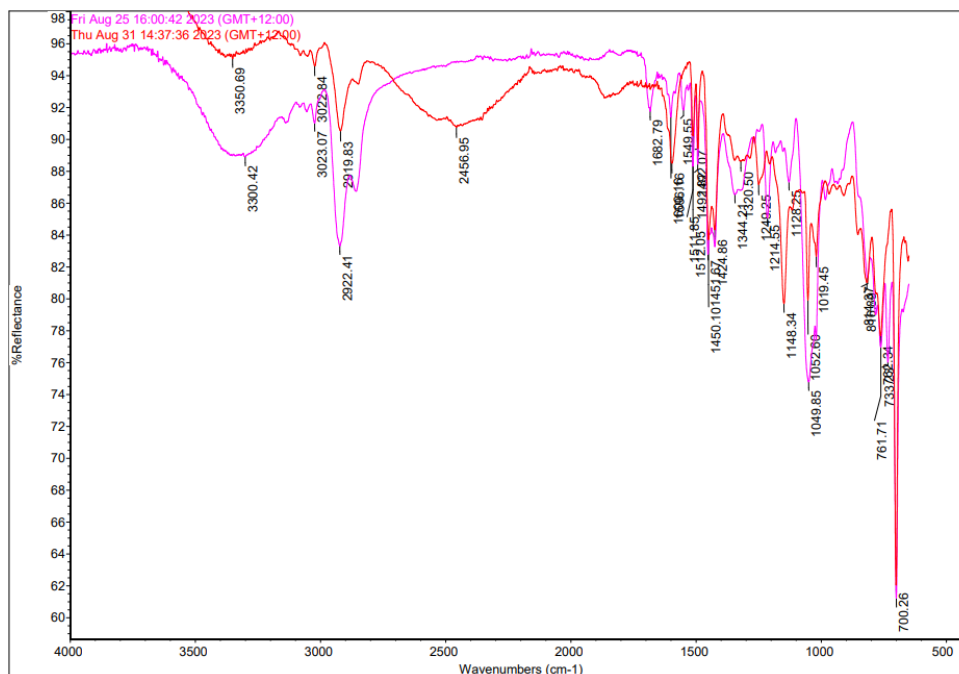


Figure 10: Post-“click” hydroxy-derivatised resin (pink) and post-“click” bromide-derivatised resin

Compound 13, designed as a model click-derivatized resin, was synthesized for the purpose of modeling and characterizing. In conjunction with this synthesis, IR spectroscopy was employed to monitor the resulting product. The resin compound was reacted with potassium phthalimide in the presence of K_2CO_3 and NaI, employing DMF as the solvent. The progression of this reaction was tracked via IR spectroscopy, and the outcomes are illustrated in Figure 11.

Upon examination of the spectra, it becomes evident that both spectra exhibit a high degree of similarity. However, in the case of the product (blue), a notable peak emerges at 1712 cm^{-1} , signifying the presence of the C=O bond characteristic of the amide derived from the phthalimide. It is important to note that there exists no peak that can definitively ascertain the completion of the reaction, specifically whether all chloride linkers have successfully reacted to completion.

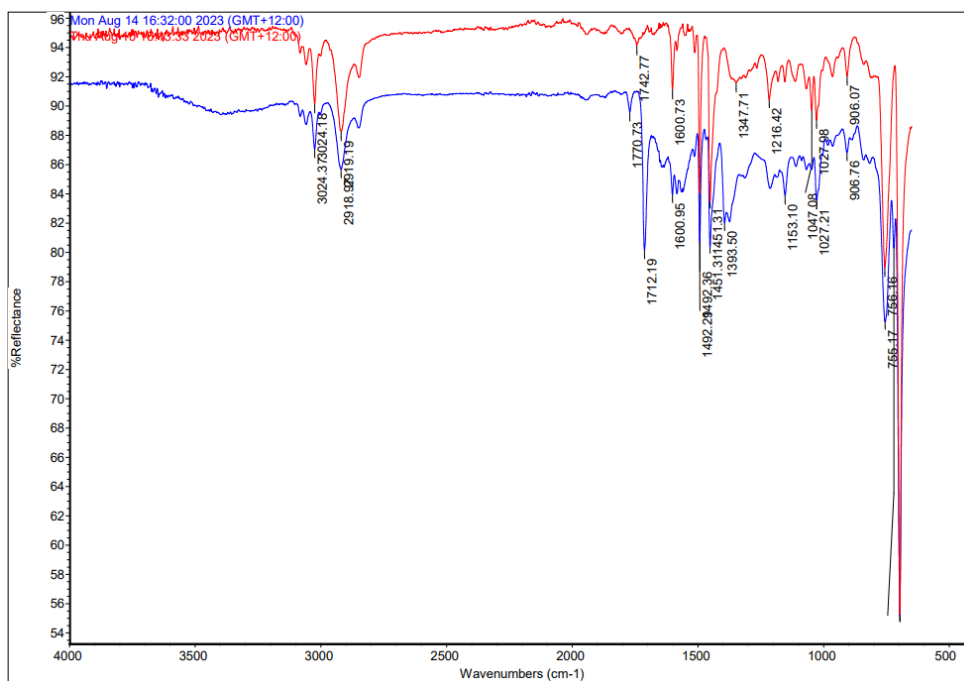


Figure 11: Model click-derivatised Merrifield resin (red) and post-“click” phthalamide-derivatised resin

Unfortunately, owing to time limitations, further exploration of this route has been put to hold. While the advantages of this approach have been highlighted, it is important to acknowledge the drawbacks, including challenges in identifying impurities and confirming the completion of reactions when, among others. With the implementation of potential optimizations, this concept may find applicability in specific synthesis processes.

2.5.0 Preliminary kinetic analysis of synthesized catalysis on HPNPP via UV-Vis

Following the successful synthesis of Merrifield resins functionalized with TACN and guanidinium ligands, the catalytic activities were assessed in the final phase of this research project. To analyze these catalytic properties, UV-Vis spectroscopy was used. The ligands, TACN and guanidinium, immobilized on the resin, were designed to create an active catalytic site for the transphosphorylation of HPNPP. HPNPP undergoes hydrolysis to produce *p*-nitrophenol, which produces a yellow-colored solution at pH 7 and can be quantified using UV absorbance spectroscopy at 405 nm. These experiments were conducted in 1 mL quartz cuvettes at a temperature of 40 degrees Celsius, and the reaction progress was continuously monitored using a UV spectrophotometer.

2.5.1 Examining the optima type of buffer and pH

A common experimental procedure involves filling a 1 mL cuvette with a selected buffer solution (5 mM), $\text{Zn}(\text{NO}_3)_2$ (ranging from 1 to 10 μM), a resin catalyst of choice (TACN or Guanidinium), and the substrate HPNP (of 500 μM). The cuvette was then filled to the top with mQ water. The concentrations of the buffer and HPNPP substrate remains at constant and variations were made in the concentration of zinc, pH levels, the choice of buffer type, and the concentration of catalysts. These adjustments were implemented to investigate the optimal conditions for the catalysts and to evaluate the resin catalysts' capability to catalyze the hydrolysis reaction.

In the initial phase of our investigation, we assessed the catalytic capabilities of TACN-derivatized resin **2^a** in catalyzing the transphosphorylation of HPNPP. Resin samples were precisely weighed and made into solution methanol to prepare a 20 nM stock solution. We opted for HEPES, an organic buffer, drawing inspiration from an established condition previously tested within our research group²⁰. For our preliminary studies, we explored pH levels of 7, 8, and 9 to gain initial insights and guide our subsequent experiments.

To evaluate the effectiveness and efficiency of the catalytic systems created by these resins, change of absorbance was monitored over time. This data enabled us to calculate the initial reaction rates. As illustrated in the figure below, it becomes evident that at pH 9, the initial rate is higher compared to pH 8 and 7. Specifically, it registers at $4.90 \times 10^{-7} \text{ M s}^{-1}$, while pH 8 and 7 exhibit rates of $2.39 \times 10^{-7} \text{ M s}^{-1}$ and $0.17 \times 10^{-7} \text{ M s}^{-1}$, respectively.

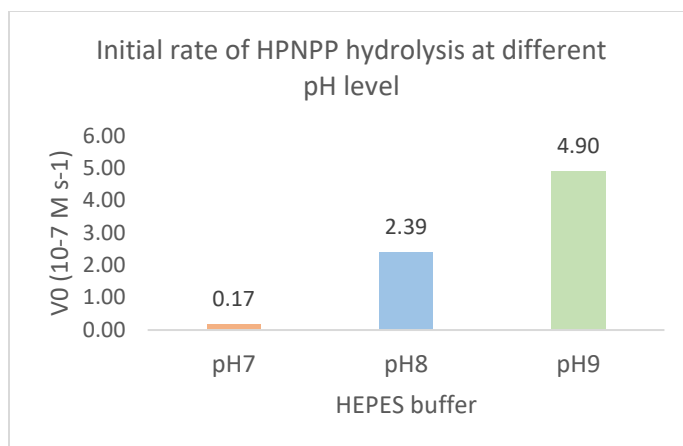


Figure 12: Initial rate of HPNPP hydrolysis at different pH level

Considering the pH levels, we proceeded to explore more into optimizing the conditions for these resins. An approach involved exploring alternative buffers at pH 9. Specifically, we tested the efficacy of another organic buffer, CHES, and an inorganic buffer, BORAX. The outcomes of these experiments are visually presented in the figure below, where compelling evidence emerged. Notably, BORAX and HEPES displayed quite comparable results, yielding reaction rates of $4.72 \times 10^{-7} \text{ M s}^{-1}$ and $4.90 \times 10^{-7} \text{ M s}^{-1}$, respectively. In contrast, CHES exhibited a slightly lower rate of $3.44 \times 10^{-7} \text{ M s}^{-1}$.

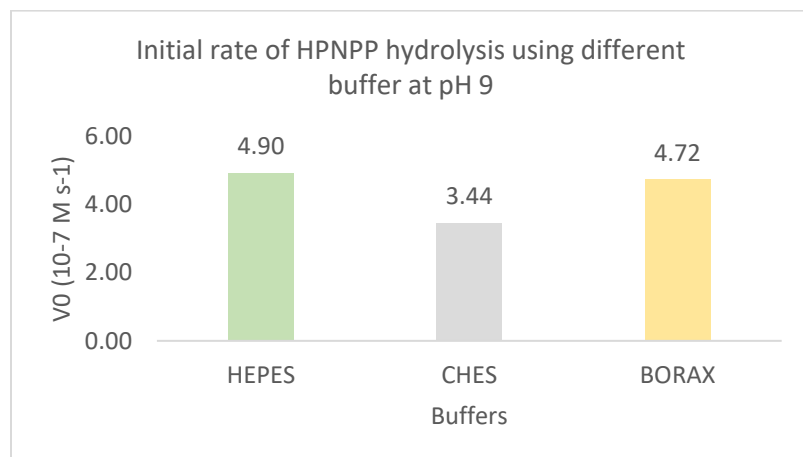


Figure 13: Initial rate of HPNPP hydrolysis using different buffer at pH 9

Considering that HEPES and BORAX produced nearly identical results, we calculated the average percentage increase in the initial rate between the resin catalyst and the blank, which contained only the buffer. These calculations revealed that HEPES exhibited an 11% increase, while BORAX demonstrated a more significant 21% increase. Therefore, we decided to further investigate the BORAX buffer.

To optimize the conditions for catalysis, we explored different pH levels of the BORAX buffer, serving as the last variable in our search for the most optimal conditions. Surprisingly, the graph displayed a better initial rate at pH 8, measuring $5.89 \times 10^{-7} \text{ M s}^{-1}$, compared to the rate of $4.72 \times 10^{-7} \text{ M s}^{-1}$ observed at pH 9. Consequently, we selected BORAX pH 8 as the preferred buffer for subsequent experiments.

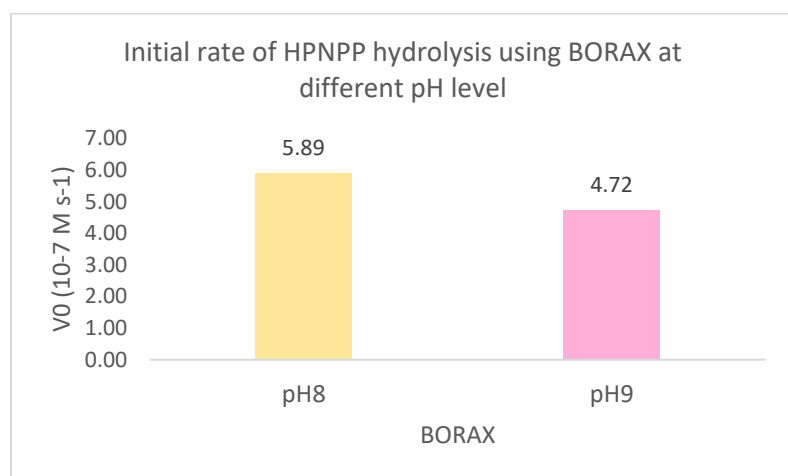


Figure 14: *Initial rate of HPNPP hydrolysis using BORAX at different pH level*

It's noteworthy that these buffer screening experiments were exclusively conducted using the TACN-derivatised resins. We assumed that the guanidinium-derivatised resins would exhibit similar behavior. Thus, under the pH 8 conditions, we also tested the guanidinium-derivatised resin with different types of buffers. Examining the graph below, it becomes evident that BORAX pH 8 consistently outperformed the other buffers, reaffirming its selection for subsequent experiments.

2.5.2 Transphosphorylation of HPNN using TACN-derivatised and Guanidinium-derivatised Merrifield resins

The catalytic activity of the resins is influenced not only by the solution's pH but also by the choice of aqueous buffer. After establishing the optimal conditions, we conducted catalytic tests on both types of resins. The primary objective of these catalysis experiments was to demonstrate that the resins indeed enhance catalysis, a narrative supported by the graphs below.

In Figure 15, we observe that in the absence of resin, which serves as the baseline, the HPNPP substrate catalyzes at a rate of $0.70 \times 10^{-7} \text{ M s}^{-1}$. In contrast, when aided by the Guanidinium-derivatised resin catalyst, the rate significantly increases to $1.69 \times 10^{-7} \text{ M s}^{-1}$, nearly two and a half times faster. Although the HPNPP hydrolysis rate remains relatively slow, these results conclusively demonstrate the impact of the Guanidinium-derivatised resin catalyst.

Examining the combination of TACN and the buffer, it becomes evident that the resin itself catalyzes the reaction in the absence of zinc at a rate of $2.27 \times 10^{-7} \text{ M s}^{-1}$. Introducing zinc to the solution leads to a substantial rate increase, exceeding twice the initial rate at $4.72 \times 10^{-7} \text{ M s}^{-1}$. While these results may not match the speed observed in our group's previous studies on the C_{16} TACN substrate¹⁶, they effectively achieve our main purpose, which is to demonstrate catalysis. Importantly, they demonstrate that catalytic groups can be immobilized onto the resin, eliminating the need for gold nanoparticles. This immobilization offers the advantage of recoverability and reuse of the catalytic material through filtration and washing.

It is crucial to emphasize that these kinetic studies on the resins represent preliminary investigations, primarily aimed at proving their catalytic capabilities. The presented results serve as compelling evidence of their catalytic potential.

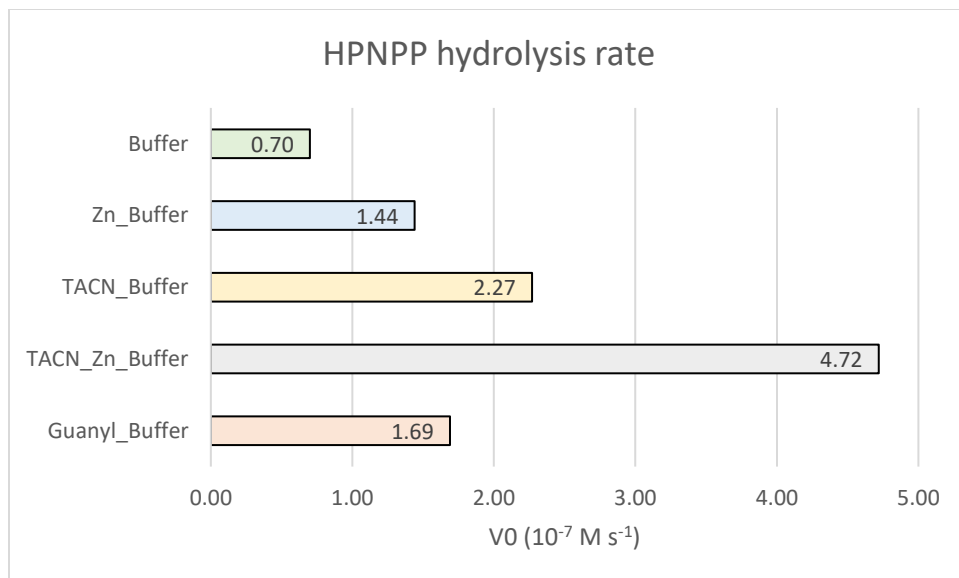


Figure 15: *HPNPP hydrolysis rate*

2.6 Conclusion and future work

In summary, this research successfully achieved the immobilization of catalytic substrates onto Merrifield resins, resulting in TACN-derivatised and Guanidinium-derivatised Merrifield resins, which demonstrated active catalytic properties in the transphosphorylation of HPNPP. The synthesis of these resins, particularly the Guanidinium-derivatised variant, posed challenges due to the compounds' volatility during the multi-step synthesis. To address this, two distinct synthetic routes were designed and implemented, leading to improved compound yields. Additionally, an alternative synthetic route was proposed, involving the immobilization of halides onto the resins, making subsequent reactions without the need for purification and overcoming the volatility issue present in other routes. Analysis of ^1H NMR and IR results from the optimized routes indicated promising improvements in synthesis efficiency. However, some optimization steps were left incomplete due to time constraints. Ideally, the proposed synthetic routes should be fully executed to calculate the overall yield and definitively demonstrate increased efficiency.

Furthermore, the immobilized catalysts were found to exhibit catalytic activity, aligning with the primary objective of this project: to immobilize catalytic substrates and confirm their efficacy. Although the system is not perfect, it proves the viability of catalysts on resins, reducing the reliance on gold nanoparticles. Future work aims to explore the co-immobilization of both Guanidinium and TACN ligands onto the same resin, achievable through the CuAAC "click" reaction. During this process, proportion optimization can be drawn from our group's prior research on C_{16} TACN on gold nanoparticles²⁰.

These findings represent the initial stages of a pathway towards creating artificial enzymes that exhibit enhanced stability compared to natural enzymes. This enhanced stability, coupled with their ease of recovery, holds significant promise for their application in various industrial processes.

CHAPTER THREE: EXPERIMENTAL

3.1 General details

Nuclear magnetic resonance (NMR) experiments were conducted using a Bruker Ascend 400 NMR spectrometer, specifically the Bruker AV400 spectrometer, operating at a frequency of 400 MHz. NMR samples were prepared in deuterated CHCl_3 and D_2O solvents, without stirring, and placed in quartz NMR tubes. The ^1H NMR spectra were recorded at a frequency of 400 MHz for ^1H nuclei, with chemical shifts (δ) reported in parts per million (ppm) and coupling constants (J) measured in Hertz (Hz).

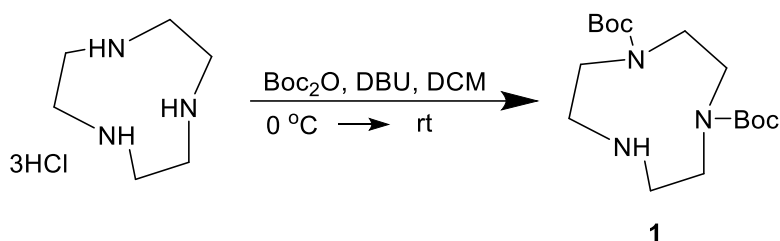
Infrared (IR) spectra were acquired using a Nicolet iS10 spectrometer, manufactured by Thermo Fisher Scientific Inc. The absorption peaks were reported in wavenumbers (cm^{-1}) and were recorded across a range of 450 to 4000 cm^{-1} . The analysis of IR spectra was conducted using OMNIC 9.2.86 software.

Ultraviolet-visible (UV-vis) spectrometer experiments were carried out using a Cary 100 UV-Vis spectrophotometer from Agilent Technologies to determine the catalytic rate. Scanning electron microscope (SEM) images were obtained using an SU-70 Schottky field emission scanning electron microscope manufactured by Hitachi, with magnifications ranging from 5K to 1.2K.

All chemicals employed as starting materials or reagents in each reaction were commercially sourced and used directly without additional purification. Ultra-pure water and DMSO solvents utilized in these experiments were obtained from Sigma-Aldrich.

3.2 Synthesis of Ligand A

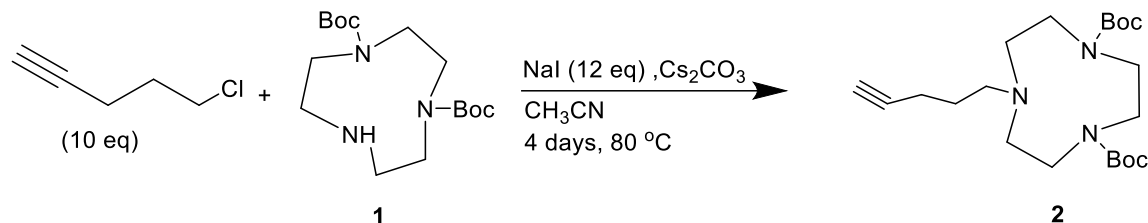
3.2.1 Synthesis of Di-*tert*-butyl 1,4,7-triazacyclononane-1,4-dicarboxylate



TACN.3HCl (500 g, 2.09 mmol) was dissolved in dry CH₂Cl₂ (10 mL) under N₂ gas. Addition of DBU (2.133 mL, 14.24 mmol) was followed and the reaction mixture was cooled down to 0 °C. Simultaneously, Boc₂O (958 g, 4.40 mmol) was dissolved using also anhydrous CH₂Cl₂ (5 mL) and was purged with N₂ gas on a different vessel. This solution was added carefully dropwise to the previous reaction mixture made using a syringe pump. The resulting mixture was stirred at room temperature for an additional 4 hours while being monitored using TLC. Unreacted materials were neutralized with sodium bicarbonate (10 mL) and was extracted with CH₂Cl₂ (3 x 10 mL). The organic layer was collected, washed with brine, and filtered through MgSO₄. The solvent was removed under reduced pressure, leaving the crude product. The crude product was purified by flash column chromatography on silica gel (MeOH/ CH₂Cl₂ 5:95 → 7:93) to yield **1** (71%) as a dark yellow oil.

¹H NMR (400 MHz, CDCl₃): δ (ppm) 3.51 – 3.44 (m, 4H), 3.32 – 3.27 (m, 4H), 2.96 (s, 4H), 1.50 (s, 18H)

3.2.2 Synthesis of di-*tert*-Butyl 7-(pent-1-yn-5-yl)-1,4,7-triazacyclononane-1,4-dicarboxylate

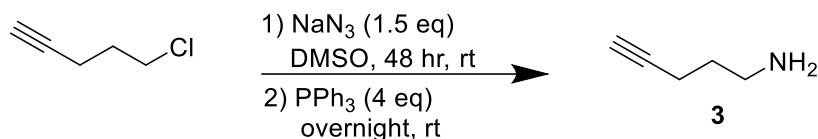


To a solution of **1** (150 mg, 0.45 mmol) in CH₃CN, NaI (818.39 mg, 5.46 mmol) and Cs₂CO₃ (146.62 mg, 0.45 mmol) were added and flushed with nitrogen to maintain the inert environment. The reaction mixture was stirred and heated to 80 °C. 5-Chloropentyne (0.48 mL, 4.55 mmol) was added carefully, and the resulting mixture was left to stir for 4 days under reflux and monitored by TLC. The reaction mixture was filtered through Celite[®], and the solvent was evaporated under reduced pressure. The crude yellow oil was purified by flash chromatography on silica gel (EtoAc/Hexane 3:7) to produce **2** 75% yield as a faint yellow oil.

¹H NMR (400 MHz, CDCl₃): δ (ppm) 3.51 – 3.46 (m, 4H), 3.30 – 3.25 (m, 4H), 2.65 – 2.58 (m, 6H), 2.25 – 2.22 (m, 2H), 1.95 (s, 1H), 1.70 – 1.64 (m, 2H) 1.49 (s, 18H)

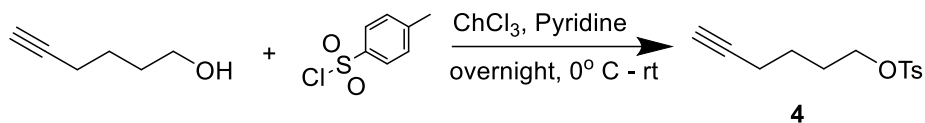
3.3.0 Synthesis of Ligand B

3.3.1 Synthesis of 5-Aminopent-1-yne



5-Chloropentyne (0.5 mL, 4.72 mmol) and NaN_3 (0.460 g, 7.08 mmol) were combined to a flask in dry DMSO (1.5 mL). The reaction mixture was stirred at room temperature to substitute the chloride group for azide and was monitored by TLC. After the reaction was stood for 48 hours, triphenyl phosphine (4.95 g, 18.88 mmol) was combined to the same vessel to reduce the azide to an amine. Additionally, 1 mL of dry DMSO was added and the reaction mixture was left overnight to stir. The crude mixture was put under freeze dry over a weekend to evaporate the excess solvent to yield **3**. Due to instability of the product, the crude material was taken directly to the next step and yield was calculated over two steps.

3.3.2 Synthesis of 6-tosylhex-1-yne

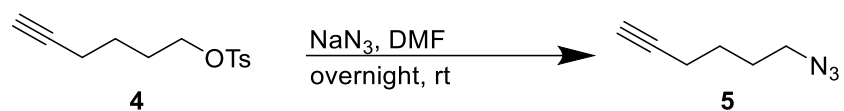


5-Hexyn-1-ol (0.5 g, 5.09 mmol) was dissolved in chloroform (3 mL), the mixture was cooled in an ice bath and purged with nitrogen gas to create an inert atmosphere. Pyridine was added to the mixture (0.82 mL, 10 mmol) and stirred. *p*-Toluenesulfonyl acid (1.40 g, 7.64 mmol) was gradually added to the mixture while stirring and maintaining the inert environment. The mixture was allowed to stir at room temperature for 24 hours.

Afterward, the resulting mixture was diluted with diethylether (10 mL) and water (5 mL) and separated. The organic layer was washed with 2M hydrochloric acid, filtered through sodium bicarbonate (NaHCO₃) and magnesium sulfate (MgSO₄), and then subjected to evaporation. This process yielded a yellow liquid, which was subsequently purified via flash chromatography on silica gel (ethyl acetate/hexane 1:10). The product identified as compound **4** was obtained with 81% yield.

¹H NMR (400 MHz, CDCl₃): δ (ppm) 7.71 – 7.68 (m, 2H), 7.28 – 7.26 (m, 2H), 3.98 – 3.95 (m, 2H), 2.36 (t, 3H), 2.36 – 1.87 (m, 2H), 2.09 (s, 1H), 1.71- 1.65 (m, 2H), 1.49 – 1.46 (m, 2H)

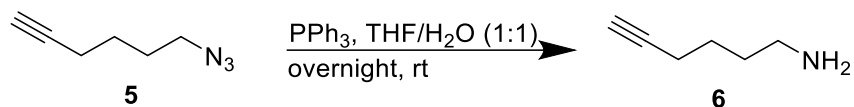
3.3.3 Synthesis of 6-azidohex-1-yne



To a solution of **4** (0.05 g, 0.198 mmol), 0.5 mL of DMF was stirred in rt and was left overnight. The reaction mixture was washed with cold deionized water and dichloromethane and no further purification was needed. Colourless liquid (**5**) was obtained in 43% yield.

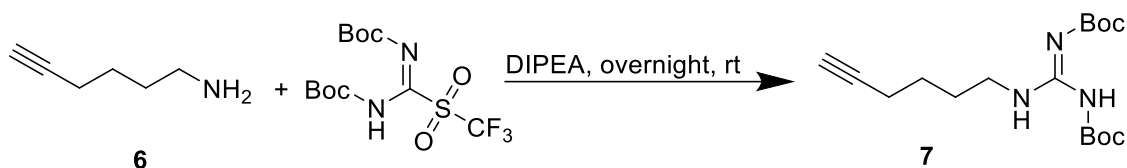
¹H NMR (400 MHz, CDCl_3): δ (ppm) 3.26 – 3.23 (t, 2H), 2.20 – 2.15 (dd, 2H), 1.91 – 1.90 (t, 1H), 1.69 – 1.55 (m, 4H)

3.3.4 Synthesis of 6-Aminohex-1-yne



Compound **5** (0.862 g, 0.7 mmol) was initially dissolved in a solution of THF/water mixture (6 mL in 1:1). Then, triphenyl phosphine was introduced into this solution, and the reaction mixture was allowed to undergo stirring in rt overnight. Following this, the solvent was removed by evaporation, and the resulting residue was diluted in 10 mL of dichloromethane. This diluted solution underwent a series of washing steps, involving 5 mL of water and 5 mL of brine, to eliminate impurities. Afterward, the organic layer was subjected to filtration through magnesium sulfate, followed by evaporation and exposure to high-pressure conditions. Notably, no further purification steps were deemed necessary, resulting in the successful isolation of Compound **6** with 78% percentage yield.

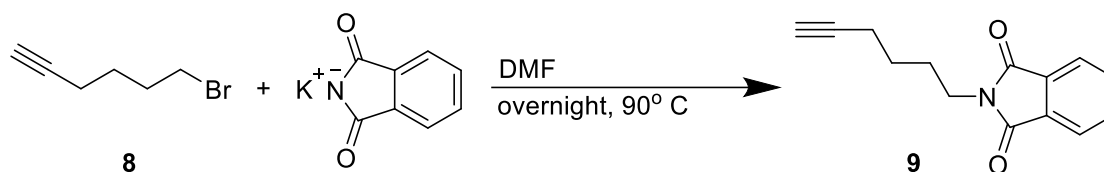
¹H NMR (400 MHz, D₂O): δ (ppm) 2.96 – 2.92 (m, 2H), 2.30 – 2.29 (t, 1H), 2.21 – 2.17 (m, 2H), 1.71 – 1.65 (m, 2H), 1.55 – 1.49 (m, 2H)

3.3.5 Synthesis of 6-(*N,N*-Bis(*tert*-butoxycarbonyl)-*N*'-butylguanidinyl)-hex-1-yne

To a solution of compound **6** (200 mg, 1.496 mmol) dissolved in 5 mL of dichloromethane, DIPEA (1.56 mL, 1.16 mmol) was added. To this mixture, N,N'-bis(*tert*-butoxycarbonyl)-*N*'-triflylguanidine (877 mg, 2.24 mmol) was introduced. The resulting reaction mixture was allowed to stir overnight and was monitored by TLC to track the progress of the reaction. Then, the reaction mixture was diluted with 5 mL of water and subjected to a series of dichloromethane washes (3 x 10 mL). The crude mixture underwent filtration, followed by evaporation. This process resulted in the formation of a slightly viscous, light-yellow liquid, which was subsequently subjected to purification through flash chromatography on silica gel (ethyl acetate/hexane 1:20). The relevant fractions were collected and subsequently evaporated, affording a yield of 50% for Compound **7**.

¹H NMR (400 MHz, CDCl₃): δ (ppm) 11.43 (s, 1H), 8.25 (s, 1H), 3.40 – 3.35 (m, 2H), 2.19 – 2.15 (m, 2H), 1.90 – 1.88 (t, 1H), 1.66 – 1.54 (m, 4H), 1.53 (s, 18H)

3.3.6 Synthesis of 2-(hex-1-yn-6-yl)phthalimide



Potassium phthalimide was introduced into a solution containing 6-bromo-1-hexyne (**8**) in DMF and stirred at room temperature. The mixture was then heated to 90 °C and allowed to stir overnight. Afterward, the mixture was cooled to room temperature before being poured into a cold-water bath (20 mL). The resulting solution was subjected to extraction with dichloromethane, and the organic layer obtained was subsequently washed with a solution of 0.2 M KOH (50 mL) and water (15 mL). The organic layer was then passed through a magnesium sulfate filter and evaporated. The resulting crude product underwent purification through flash column chromatography on silica gel (ethyl acetate/hexane 1:5), and relevant fractions were collected. This process resulted in a 78% yield of Compound **9**.

¹H NMR (400 MHz, CDCl₃): δ (ppm) 7.79 – 7.76 (dd, 2H), 7.65 – 7.63 (dd, 2H), 3.66 – 3.63 (t, 2H), 2.20 – 2.16 (m, 2H), 1.90 – 1.87 (m, 1H), 1.77 – 1.71 (m, 2H), 1.55 – 1.51 (m, 4H)

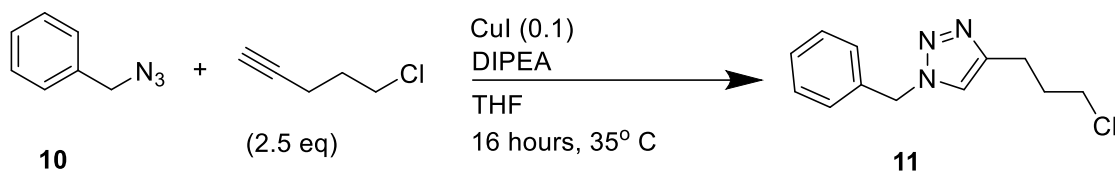
3.4.0 Synthesis of Merrifield resins, click reactions and deprotections

3.4.1 Synthesis of benzyl azide



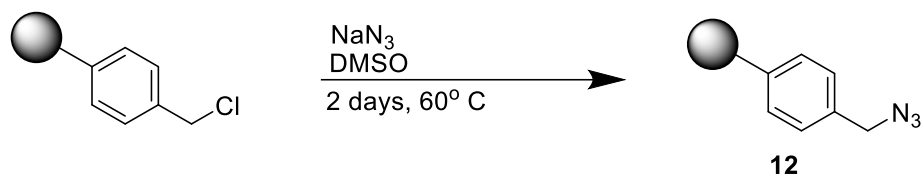
Benzyl bromide (0.34 mL, 3.95 mmol) was dissolved in 5 mL of dimethyl sulfoxide (DMSO). Subsequently, sodium azide (385 mg, 5.92 mmol) was introduced into the mixture, and the solution was allowed to stir at room temperature for 24 hours. Following this period, the mixture was diluted with cold water and subjected to extraction using dichloromethane (3 x 10 mL). The resulting crude mixture was then passed through a magnesium sulfate filter and then evaporated and concentrated under reduced pressure. No additional purification steps were necessary, yielding Product **10** at a 60% yield.

3.4.2 Synthesis of 1-benzyl-4-(1-chloropro-3-ynyl)-1,2,3-triazole



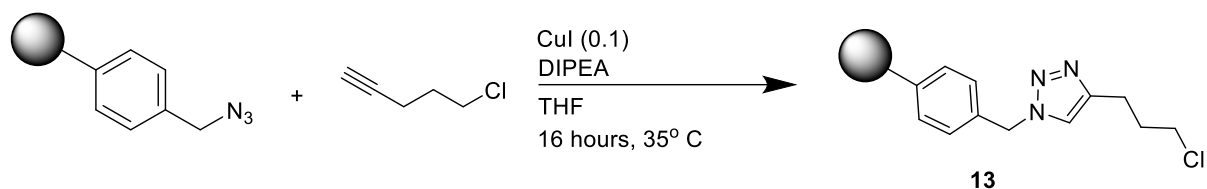
To a solution of benzyl azide (100 mg, 0.75 mmol) dissolved in anhydrous THF (5 mL), CuI (91.4 mg, 0.075 mmol) was added and the flask was flushed with nitrogen gas to keep an inert environment. Then, 5-chloropentyne (192.50 mg, 1.87 mmol) was added to the mixture, followed by the controlled addition of DIPEA (0.5 mL, 0.3 mmol). The reaction mixture was heated to 35 °C and was left to stir under reflux for 16 hours and was followed by TLC. The resulting mixture was extracted with dichloromethane and evaporated to obtain product **11**.

A solution containing benzyl azide (100 mg, 0.75 mmol) dissolved in anhydrous tetrahydrofuran (THF) (5 mL) was prepared. CuI was introduced into the solution, and the flask was purged with nitrogen gas to maintain an inert environment. Then, 5-chloropentyne (192.50 mg, 1.87 mmol) was added to the mixture, followed by the gradual addition of DIPEA (0.5 mL, 0.3 mmol). The reaction mixture was heated to 35 °C and allowed to reflux for 16 hours, during which it was monitored by thin-layer chromatography (TLC). Following the completion of the reaction, the resulting mixture was extracted with dichloromethane (3 x 10 mL) and subsequently evaporated to yield Product **11**.

3.4.3 Synthesis of Azide-derivatised Merrifield resin (azidomethyl polystyrene)

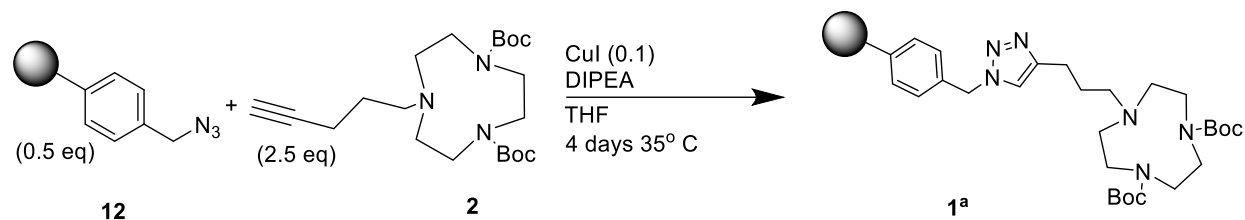
Merrifield resin (1 g, 1.1-1.7 mmol/g) was soaked in dimethyl sulfoxide (15 mL) first for 10 minutes, before the addition of sodium azide (5eq). The reaction mixture was then put under reflux and heated to 60°C and was left to agitate for 48 hours. Then, the reaction was left to cool to rt and was filtered. The filtrated resin was alternatively washed with MeOH (3 x 15 mL) and CH_2Cl_2 (3 x 15 mL) to give the desired product, azide-derivatised Merrifield resin (**12**) at 43% yield.

3.4.4 Synthesis of Model click-derivatised Merrifield resin



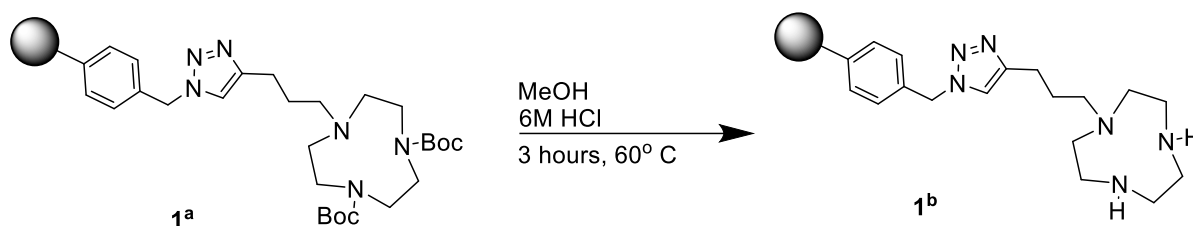
Azide-derivatised Merrifield resin (50 mg, 1.1-1.7 mmol/g) was immersed in 10 mL of tetrahydrofuran (THF) and purged with nitrogen gas to create an inert atmosphere. Subsequently, CuI (3 mg, 0.015 mmol) was introduced into the flask, followed by the addition of DIPEA (0.01 mL, 0.06 mmol), and lastly, 5-chloropentyne (37.94 mg, 0.37 mmol). The reaction mixture was then heated to 35°C and allowed to reflux for 16 hours with agitation. The resulting mixture yielded yellow/brown resins, which were separated by filtration through a filter funnel. The resins were thoroughly washed with pyridine, methanol, and dichloromethane. Following the solvent evaporation step, Product **13** was obtained.

3.4.5 Synthesis diBocTACN-derivatised Merrifield resin



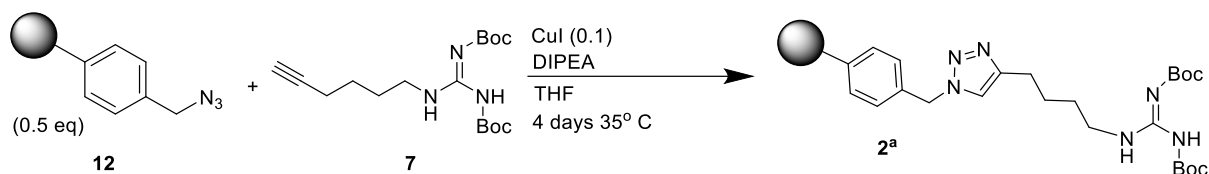
Azide-derivatised Merrifield resin (0.022 g, 1.1-1.7 mmol/g) was soaked in 10 mL of tetrahydrofuran (THF) and purged with nitrogen gas to establish an inert atmosphere. Then, CuI (1.9 mg, 0.01 mmol) was introduced into the flask, followed by the addition of DIPEA (0.008 mL, 0.048 mmol), and finally, di-tert-Butyl 7-(pent-1-yn-5-yl)-1,4,7-triazacyclononane-1,4-dicarboxylate (120 mg, 0.30 mmol). The reaction mixture was then heated to 35 °C and allowed to reflux for 4 days with agitation. The resulting mixture yielded yellow resins, which were separated by filtration through a filter funnel. The resins were thoroughly washed with pyridine, methanol, and dichloromethane. Following the solvent evaporation step, product 1a was obtained.

3.4.6 Synthesis of TACN-derivatised Merrifield resin



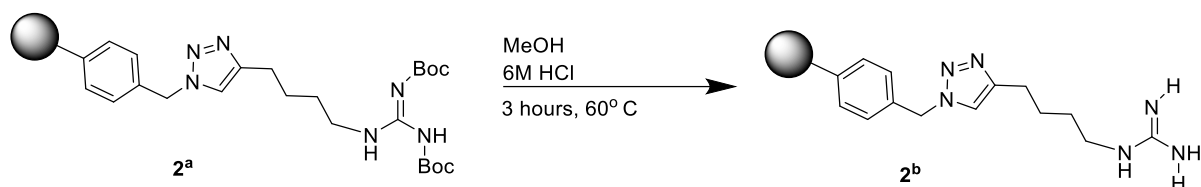
Compound **1a** (40 mg, 1.1-1.7 mmol/g) was put in a flask and soaked in methanol (MeOH) for 10 minutes. Following, 6M HCl (3 mL) was introduced into the solution, and the reaction mixture was heated to 60 °C, stirring for 4 hours. Following this, the mixture was cooled to room temperature, and the resultant solution was subjected to filtration. The remaining solid residue underwent a concurrent wash with water, MeOH, and dichloromethane. Excess solvents were then evaporated, to obtain **1b**.

3.4.7 Synthesis of diBoc-guanidinium-derivatised Merrifield resin



Azide-derivatized Merrifield resin (0.25 g, 1.1-1.7 mmol/g) was immersed in 10 mL of tetrahydrofuran (THF) and purged with nitrogen gas to establish an inert atmosphere. Then, CuI (2.6 mg, 0.014 mmol) was introduced into the flask, followed by the addition of DIPEA (0.01 mL, 0.56 mmol), and finally, 6-(N,N'-Bis(tert-butoxycarbonyl)-N''-butylguanidiny)-hex-1-yne (120 mg, 0.35 mmol). The reaction mixture was then heated to 35 °C and allowed to reflux for 4 days with agitation. The resulting mixture yielded yellow resins, which were separated by filtration through a filter funnel. The resins were thoroughly washed with pyridine, methanol, and dichloromethane. Following the solvent evaporation step, product **2a** was obtained.

3.4.8 Synthesis Guanidinium-derivatised Merrifield resin



Compound **2a** (70 mg, 1.1-1.7 mmol/g) was placed in a flask and soaked in methanol (MeOH) for 10 minutes. Then, 6M HCl (5 mL) was introduced into the solution, and the reaction mixture was heated to 60 °C, stirring for 3 hours. Following this, the mixture was cooled to room temperature, and the resulting solution was filtered. The remaining solid residue underwent a simultaneous wash with water, MeOH, and dichloromethane. Excess solvents were then evaporated, to obtain **2b**.

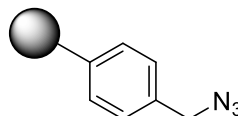
REFERENCE

1. Fechete, Ioana, Ye Wang, and Jacques C. Védrine. "The past, present and future of heterogeneous catalysis." *Catalysis Today* 189, no. 1 (2012): 2-27.
2. Nguyen, Thanh Nhat, Thuy Tran Phuong Nhat, Ken Takimoto, Ashutosh Thakur, Shun Nishimura, Junya Ohyama, Itsuki Miyazato et al. "High-throughput experimentation and catalyst informatics for oxidative coupling of methane." *ACS Catalysis* 10, no. 2 (2019): 921-932.
3. Wolfenden, Richard, and Mark J. Snider. "The depth of chemical time and the power of enzymes as catalysts." *Accounts of chemical research* 34, no. 12 (2001): 938-945.
4. Whitcomb, David C., and Mark E. Lowe. "Human pancreatic digestive enzymes." *Digestive diseases and sciences* 52 (2007): 1-17.
5. Thummel, Kenneth E., Kent L. Kunze, and Danny D. Shen. "Enzyme-catalyzed processes of first-pass hepatic and intestinal drug extraction." *Advanced drug delivery reviews* 27, no. 2-3 (1997): 99-127.
6. Vasconcelos, Andreia, Carla JSM Silva, Marc Schroeder, Georg M. Guebitz, and Artur Cavaco-Paulo. "Detergent formulations for wool domestic washings containing immobilized enzymes." *Biotechnology letters* 28 (2006): 725-731.
7. Begley CG, Paragina S, Sporn A (1990) An analysis of contact lens enzyme cleaners
8. Riva, Sergio. "Laccases: blue enzymes for green chemistry." *TRENDS in Biotechnology* 24, no. 5 (2006): 219-226.
9. Swiegers, Gerhard F., Jun Chen, and Pawel Wagner. "Bioinspired catalysis." *Bioinspiration and Biomimicry in Chemistry: Reverse-Engineering Nature* (2012): 165-208.
10. (a) Breslow, R. *Acc. Chem. Res.* 1995, 28, 146; (b) Breslow, R. *Chem. Soc. Rev.* 1972, 1, 553; (c) See also Breslow, R.; Dong, S. D. *Chem. Rev.* 1998, 98, 1997.
11. Bertini, Ivano, ed. *Biological inorganic chemistry: structure and reactivity*. University Science Books, 2007.
12. Lipscomb, William N., and Norbert Sträter. "Recent advances in zinc enzymology." *Chemical Reviews* 96, no. 7 (1996): 2375-2434.
13. Prins, Leonard J. "Emergence of complex chemistry on an organic monolayer." *Accounts of Chemical Research* 48, no. 7 (2015): 1920-1928.

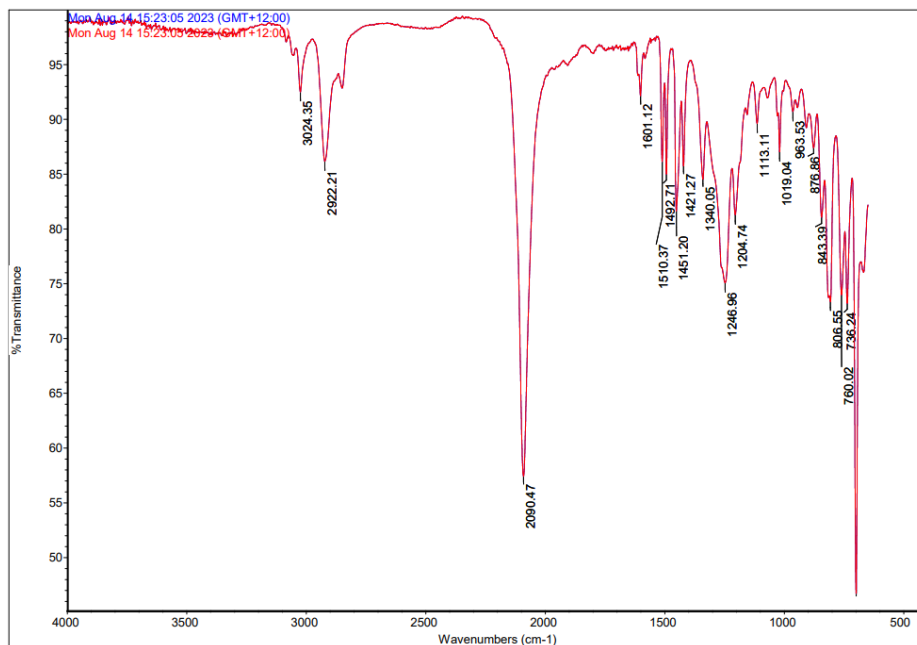
14. Mancin, Fabrizio, Paolo Scrimin, Paolo Tecilla, and Umberto Tonellato. "Amphiphilic metalloaggregates: Catalysis, transport, and sensing." *Coordination Chemistry Reviews* 253, no. 17-18 (2009): 2150-2165.
15. Mancin, Fabrizio, Leonard J. Prins, Paolo Pengo, Lucia Pasquato, Paolo Tecilla, and Paolo Scrimin. "Hydrolytic metallo-nanozymes: From micelles and vesicles to gold nanoparticles." *Molecules* 21, no. 8 (2016): 1014.
16. Solís Muñana, Pablo, Giulio Ragazzon, Julien Dupont, Chloe Z-J. Ren, Leonard J. Prins, and Jack L-Y. Chen. "Substrate-induced self-assembly of cooperative catalysts." *Angewandte Chemie International Edition* 57, no. 50 (2018): 16469-16474.
17. Rebilly, Jean-Noël, Benoit Colasson, Olivia Bistri, Diana Over, and Olivia Reinaud. "Biomimetic cavity-based metal complexes." *Chemical Society Reviews* 44, no. 2 (2015): 467-489.
18. Wulff, Günter, and Junqiu Liu. "Design of biomimetic catalysts by molecular imprinting in synthetic polymers: the role of transition state stabilization." *Accounts of chemical research* 45, no. 2 (2012): 239-247.
19. Manea, Flavio, Florence Bodar Houillon, Lucia Pasquato, and Paolo Scrimin. "Nanozymes: Gold-nanoparticle-based transphosphorylation catalysts." *Angewandte Chemie International Edition* 43, no. 45 (2004): 6165-6169.
20. Ren, C. Z. J., Solis-Munana, P., Warr, G. G., & Chen, J. L. Y. (2020). Dynamic and modular formation of a synergistic transphosphorylation catalyst. *ACS Catalysis*, 10(15), 8395-8401.
21. Salvio, Riccardo, and Antonio Cincotti. "Guanidine based self-assembled monolayers on Au nanoparticles as artificial phosphodiesterases." *RSC advances* 4, no. 54 (2014): 28678-28682.
22. Blondeau, Pascal, Margarita Segura, Ruth Pérez-Fernández, and Javier de Mendoza. "Molecular recognition of oxoanions based on guanidinium receptors." *Chemical Society Reviews* 36, no. 2 (2007): 198-210.
23. Salvio, Riccardo. "The guanidinium unit in the catalysis of phosphoryl transfer reactions: From molecular spacers to nanostructured supports." *Chemistry—A European Journal* 21, no. 31 (2015): 10960-10971.
24. Merrifield, Robert Bruce. "Solid phase synthesis (Nobel lecture)." *Angewandte Chemie International Edition in English* 24, no. 10 (1985): 799-810

Appendices

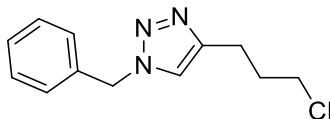
Azide-derivatised Merrifield resin



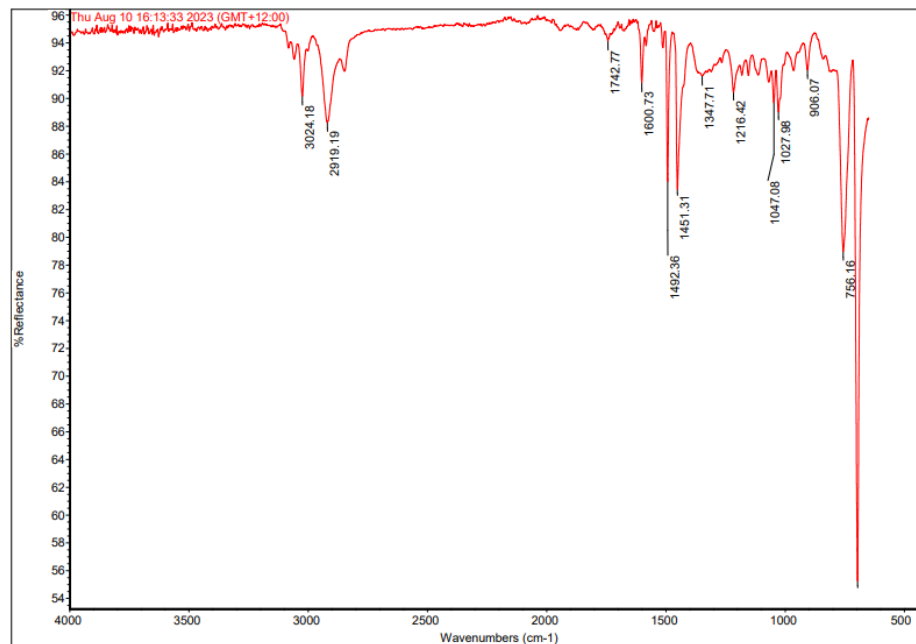
IR spectrum:



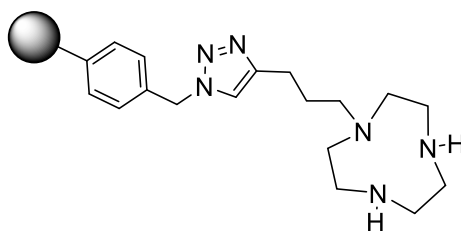
Model click-derivatised Merrifield resin



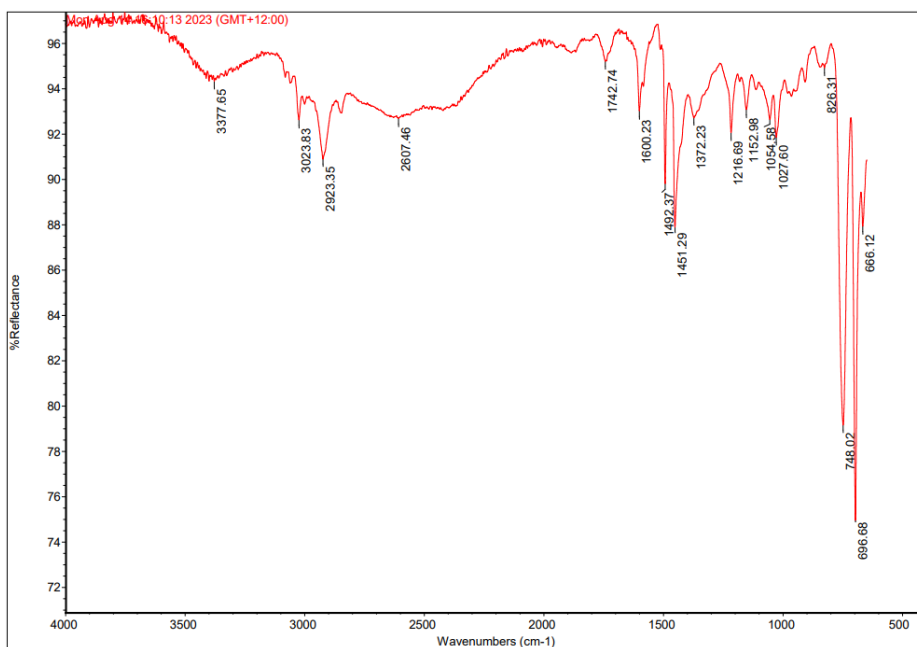
IR spectrum:



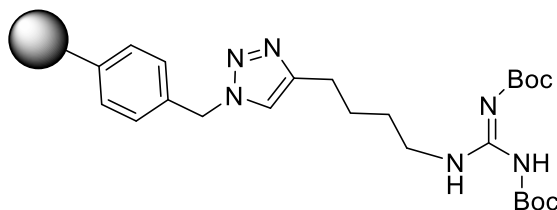
TACN-derivatised Merrifield resin



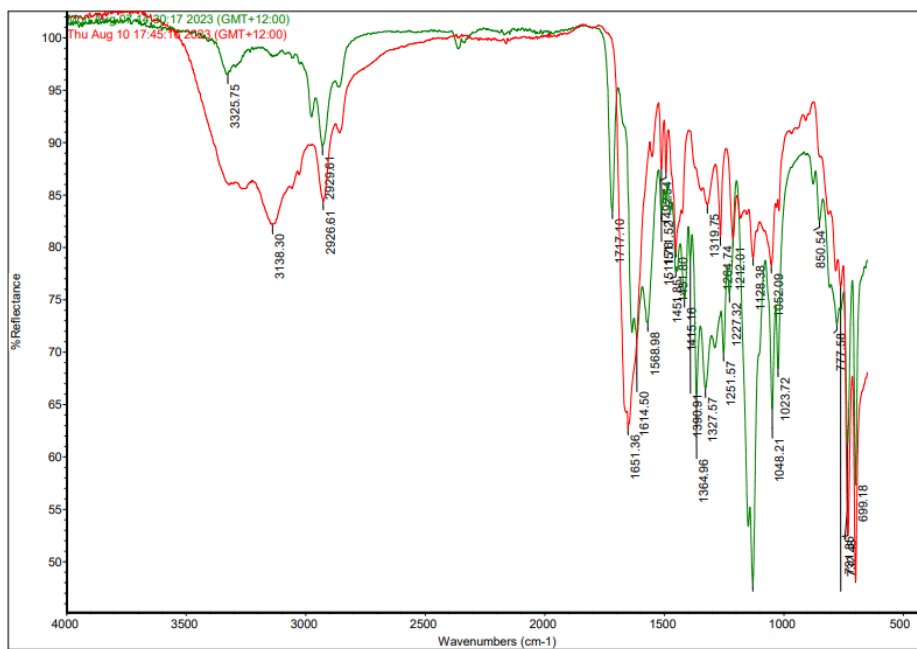
IR spectrum:



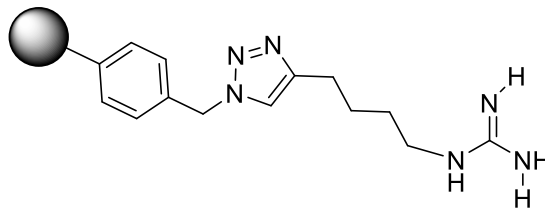
DiBoc-guanidinium-derivatised Merrifield resin (green colour)



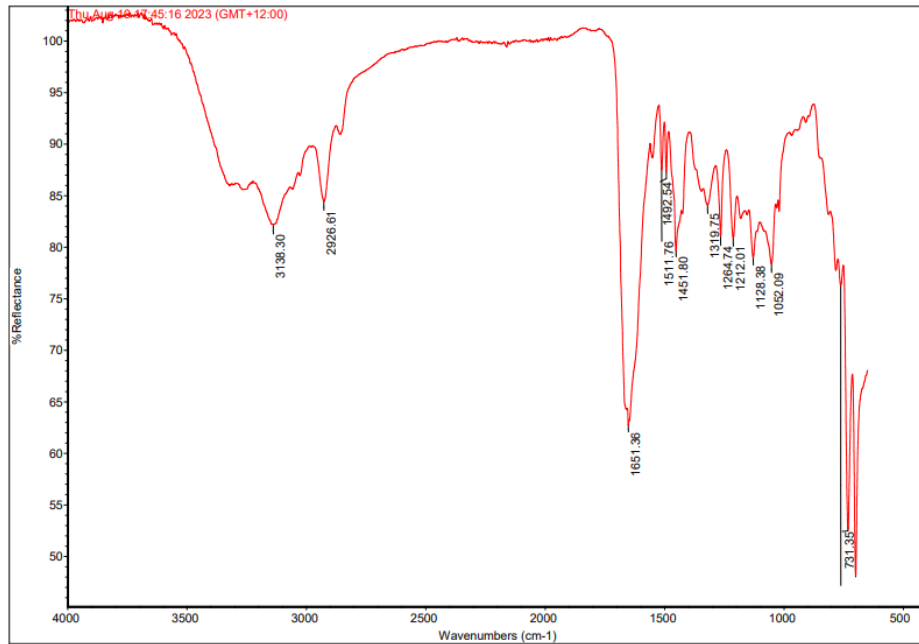
IR spectrum:



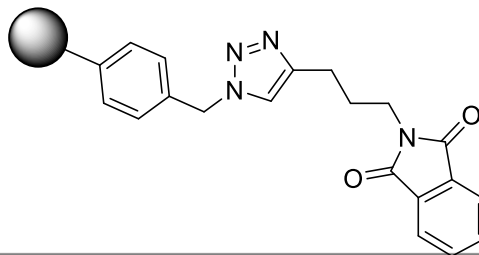
Guanidinium-derivatised Merrifield resin



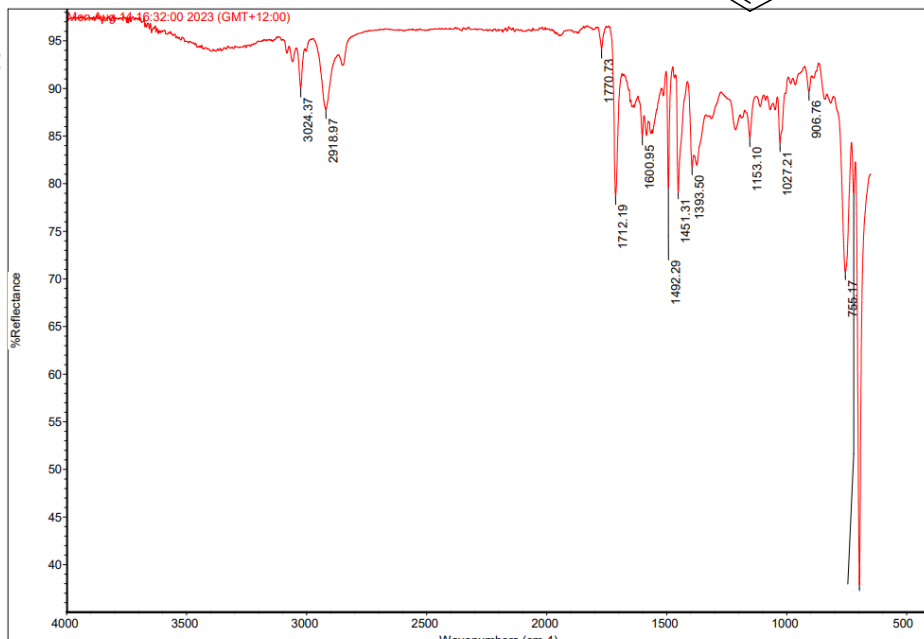
IR spectrum:



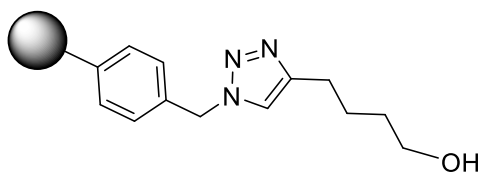
Phthalimide derivitised Merrifield resin



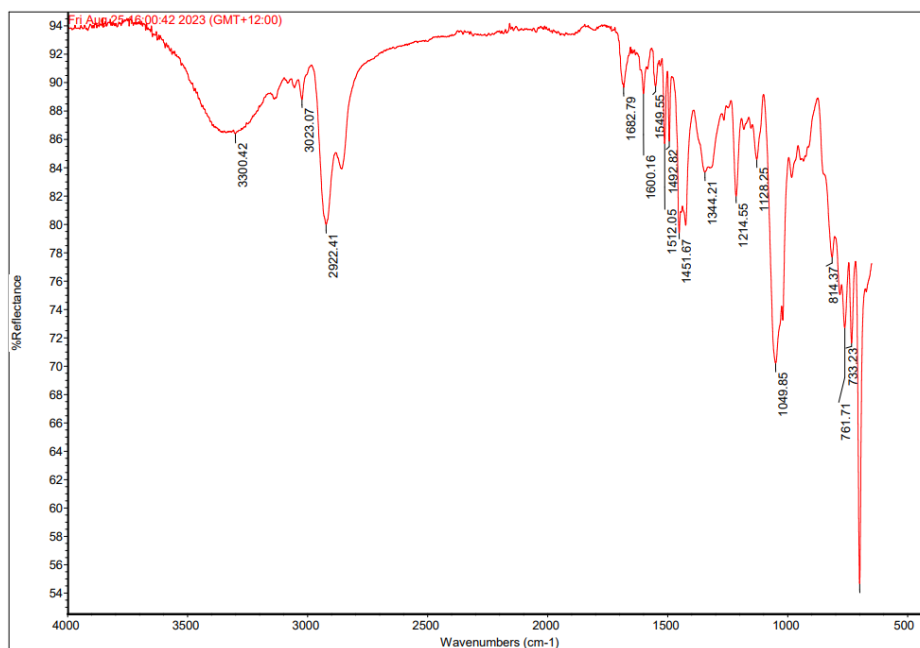
IR spectrum:



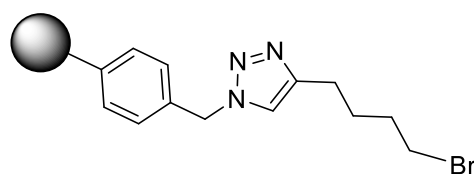
Hydroxy derivitised Merrifield resin



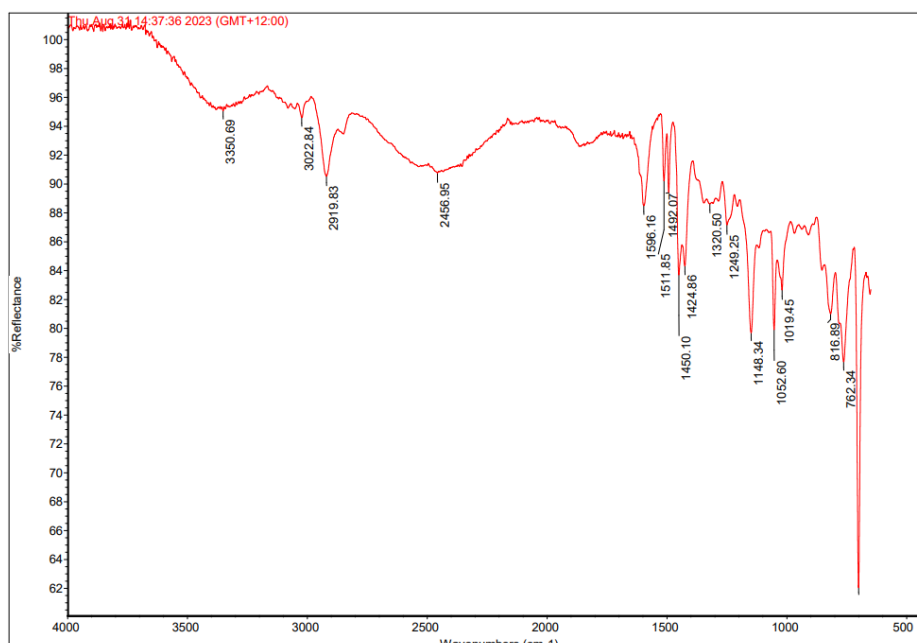
IR spectrum:



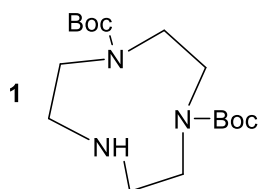
Bromide derivitised Merrifield resin



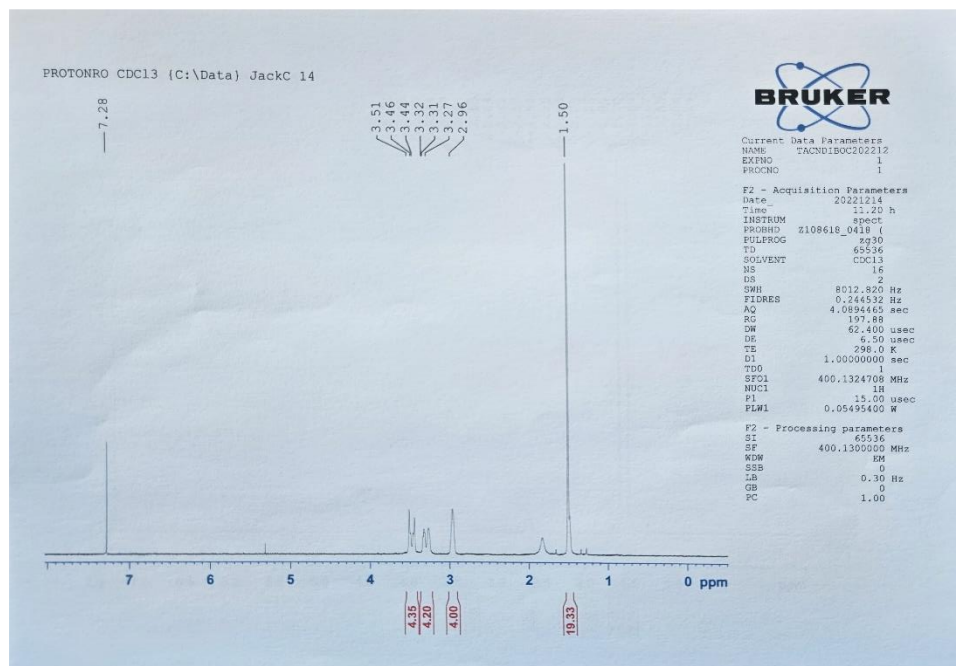
IR spectrum::



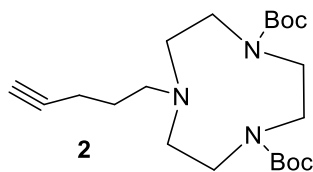
Di-*tert*-butyl 1,4,7-triazacyclononane-1,4-dicarboxylate



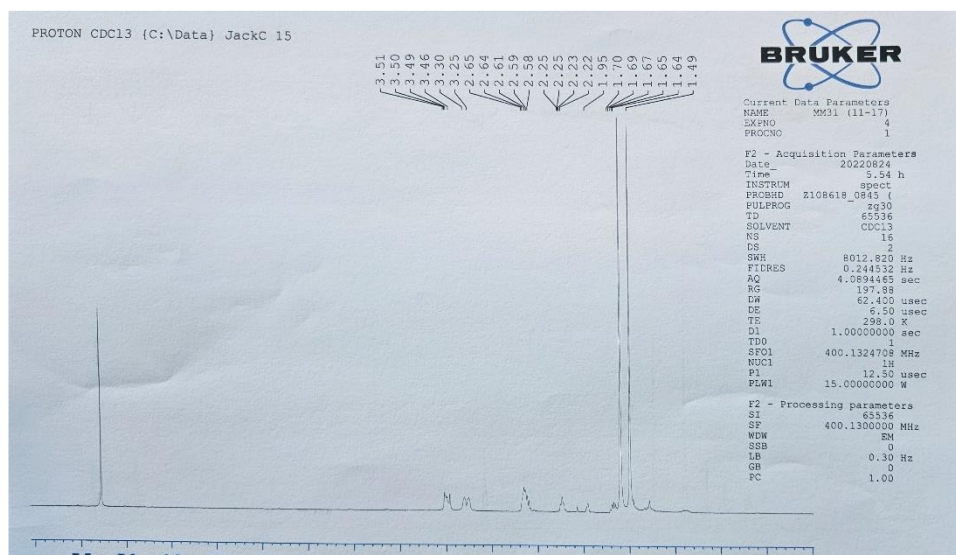
¹H NMR:



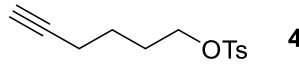
Di-*tert*-Butyl 7-(pent-1-yn-5-yl)-1,4,7-triazacyclononane-1,4-dicarboxylate



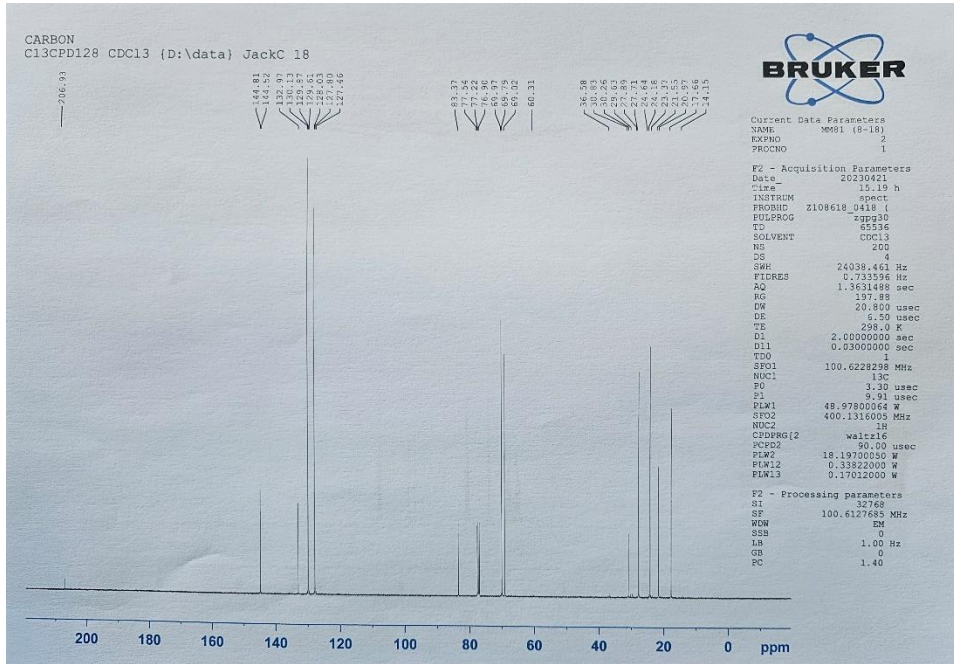
¹H NMR:



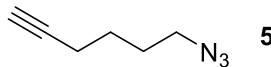
6-tosylhex-1-yne **4**



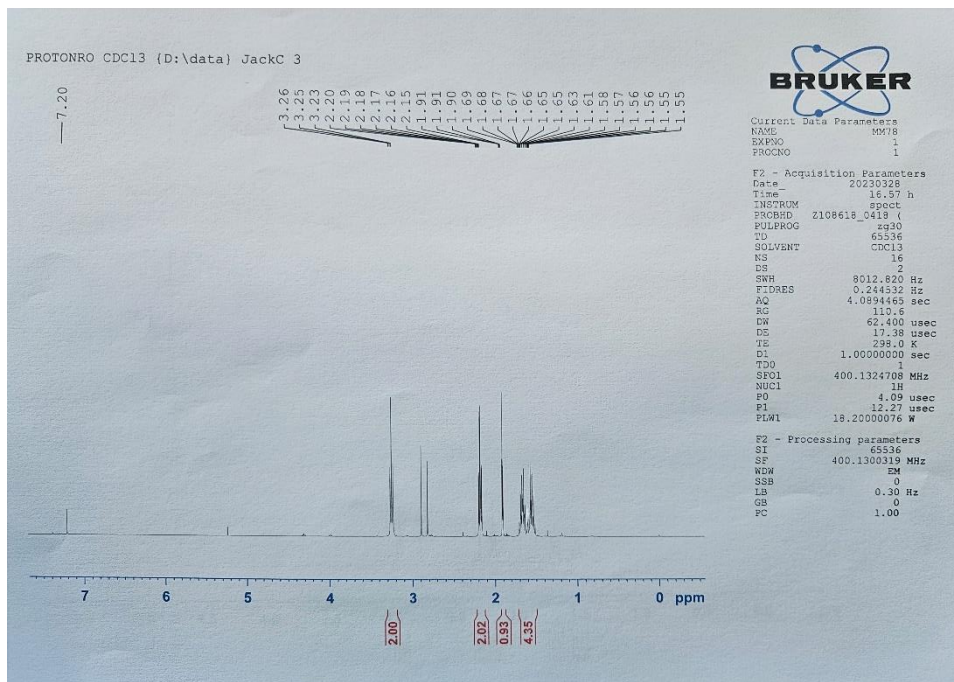
¹H NMR:



6-azidohex-1-yne **5**

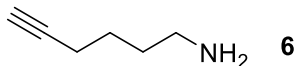


¹H NMR:

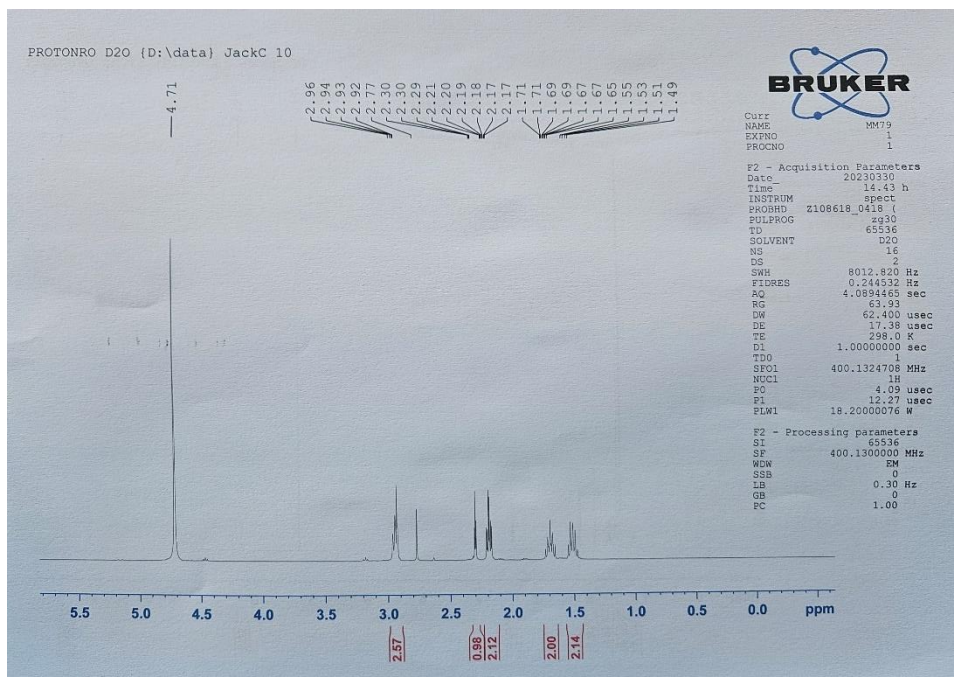


Honours Dissertation

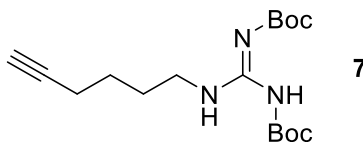
6-Aminohex-1-yne



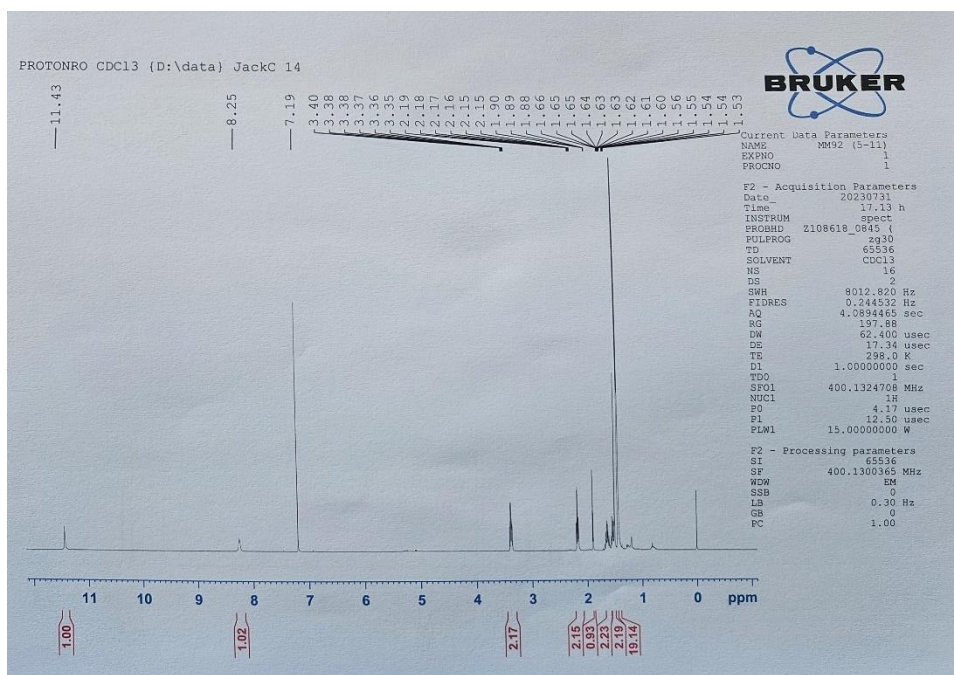
¹H NMR:



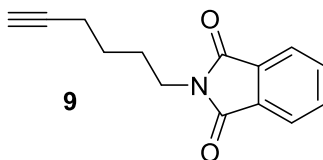
6-(*N,N*-Bis(*tert*-butoxycarbonyl)-*N'*-butylguanidinyl)-hex-1-yne



¹H NMR:



2-(Hex-1-yn-6-yl)phthalimide



¹H NMR:

